

# Guided sequential ABC schemes for intractable Bayesian models

Umberto Picchini<sup>1\*</sup>, Massimiliano Tamborrino<sup>2</sup>

<sup>1</sup> Department of Mathematical Sciences, Chalmers University of Technology and the University of Gothenburg, Sweden.

<sup>2</sup> Department of Statistics, University of Warwick, UK.

## Abstract

Sequential algorithms such as sequential importance sampling (SIS) and sequential Monte Carlo (SMC) have proven fundamental in Bayesian inference for models not admitting a readily available likelihood function. For approximate Bayesian computation (ABC), sequential Monte Carlo ABC is the state-of-art sampler. However, since the ABC paradigm is intrinsically wasteful, sequential ABC schemes can benefit from well-targeted proposal samplers that efficiently avoid improbable parameter regions. We contribute to the ABC modeller’s toolbox with novel proposal samplers that are conditional to summary statistics of the data. In a sense, the proposed parameters are “guided” to rapidly reach regions of the posterior surface that are compatible with the observed data. This speeds up the convergence of these sequential samplers, thus reducing the computational effort, while preserving the accuracy in the inference. We provide a variety of guided samplers for both SIS-ABC and SMC-ABC easing inference for challenging case-studies, including hierarchical models with high-dimensional summary statistics (21 parameters to infer using 180 summaries) and a simulation study of cell movements (using more than 400 summaries).

**Keywords:** approximate Bayesian computation; intractable likelihoods; likelihood-free; sequential Monte Carlo.

## 1 Introduction

Approximate Bayesian computation (ABC) is arguably the most popular family of Bayesian samplers for statistical models characterized by intractable likelihood functions (Sisson et al., 2018). By this, we refer to many scenarios where the likelihood  $p(y|\theta)$ , for a dataset  $y \in \mathcal{Y}$  and parameter  $\theta$ , is not available in closed-form or may be too cumbersome to evaluate computationally or even approximate. However, it could be feasible to simulate from the data-generating model to produce an artificial/synthetic dataset  $z \sim p(z|\theta)$ . The latter notation means that  $z \in \mathcal{Y}$  has been implicitly generated by the likelihood function. That is,  $p(z|\theta)$  is unavailable in closed form, but we can obtain simulated data  $z$  from it. When the time to generate many simulated dataset is not prohibitive, ABC samplers exploit the information brought by many simulated dataset at different values of  $\theta$  to learn an approximation of the posterior distribution. This is attained by comparing the several simulated dataset  $z$  with the observed  $y$ , possibly by first reducing the data-dimension via informative summary statistics, and rejecting the values of  $\theta$  yielding simulated data that are too different from the observations.

Among all ABC algorithms, those based on sequential important sampling (SIS) and especially sequential Monte Carlo (SMC) are the gold-standard. For example, SMC-ABC is the algorithm of choice in recent inference platforms such as ABCpy (Dutta et al., 2017) and pyABC (Schälte et al., 2022). However, ABC algorithms are generally computationally wasteful, making their use computationally challenging when simulating complex systems. The goal of this work is to construct novel proposal samplers for sequential ABC algorithms which are “guided” to target the observed data and hence

---

\*picchini@chalmers.se

reduce the computational effort, compared to non-guided proposals. The most basic ABC sampler is the so-called ABC-rejection sampler. This typically compares *features* of the simulated and observed data, by introducing summary statistics  $S$  which reduce the dimension of  $z$  as well as  $y$  via  $s := S(z)$  and  $s_y := S(y)$ , respectively (Pritchard et al., 1999). Ultimately,  $s$  is compared to  $s_y$ , rather than comparing  $z$  and  $y$  directly, via a distance  $\|s - s_y\|$  or a function thereof via the introduction of a kernel function  $K(\|s - s_y\|)$ , see, e.g. Sisson et al., 2018. As an example, the ABC-rejection sampler works as follows: (i) a candidate parameter  $\theta^*$  is proposed from the prior  $\pi(\theta)$ , (ii) corresponding simulated data are obtained as  $z \sim p(z|\theta^*)$ , and summaries  $s^* = S(z^*)$  are obtained. (iii) If  $\|s^* - s_y\| < \delta$ , for some  $\delta > 0$ ,  $\theta^*$  is accepted and stored, otherwise it is discarded. Steps (i-iii) are iterated until  $N$  accepted parameters are obtained. For the reader’s benefit, a more general version of this algorithm is given in Supplementary Material. Accepted draws from ABC-rejection are actually samples from the joint ABC posterior

$$\pi_\delta(\theta, s|s_y) \propto \mathbb{I}_{\|s - s_y\| < \delta} \cdot p(s|\theta)\pi(\theta),$$

(with  $\mathbb{I}_A$  the indicator function returning 1 if  $A$  is true and 0 otherwise) but we are typically only interested in retaining the accepted parameters, which are samples from the marginal posterior  $\pi_\delta(\theta|s_y) \propto \int \mathbb{I}_{\|s - s_y\| < \delta} \cdot p(s|\theta)\pi(\theta)ds$ .

The ABC-rejection sampler is particularly wasteful when the space  $\mathcal{Y}$  of observed and simulated data is continuous, or when the information encoded into the prior is vague and very different from the posterior one. A number of improvements to this basic algorithm has been produced in the past 20 years and are considered in Sisson et al. (2018). The most important alternative samplers are Markov chain Monte Carlo (MCMC) ABC (Marjoram et al., 2003; Sisson and Fan, 2011) and sequential Monte Carlo ABC (SMC-ABC, Sisson et al., 2007, Beaumont et al., 2009, Del Moral et al., 2012), where the latter is especially popular due to its somehow simpler setup compared to MCMC-ABC.

In this work, we focus on sequential ABC strategies, namely sequential importance sampling ABC (SIS-ABC) and SMC-ABC. Our contribution is the construction of several proposal functions, for both SIS-ABC and SMC-ABC, generating parameters  $\theta^*$  conditionally to  $s_y$ , with the goal of reducing the computational effort, especially in the initial iterations, by avoiding the exploration of highly unlikely parameter regions. We construct Gaussian and copula-based proposal functions, and call them “guided proposals”, due to the conditioning on  $s_y$ , and show how to allow proposed parameters to be guided towards high posterior probability regions, while correcting for possibly poor exploration of the posterior surface.

Previous work exploiting information from data summaries  $s_y$  to adjust the output of an ABC procedure is, e.g., Beaumont et al. (2002), Blum and François (2010) and Li et al. (2017)). However, these approaches do not use  $s_y$  to improve the *proposal* sampler while the ABC procedure is running, but only adjust the final output, thus acting on the already accepted parameters. Instead, our approaches make use of  $s_y$  to guide the parameter proposals while ABC is running. A similar work in this direction is Chen and Gutmann (2019), where “regression adjustment” (Beaumont et al., 2002, Blum and François, 2010) is performed by employing neural networks trained via early-stopping. The approach in Chen and Gutmann (2019) can be summarised as follows: (a) obtain proposed parameters  $\theta^{(i)}$  and corresponding simulated summaries  $s^{(i)}$  simulated via the prior-predictive distribution, then regression-adjust the former as  $\theta^{(i)'} = g(s_y) + \theta^{(i)} - g(s^{(i)})$ , where  $g(\cdot)$  is a function learned by training a neural-network on the prior-predictive simulations; (b) using the subset of  $\theta^{(i)'}$  generating small distances, construct a multivariate Gaussian sampler with mean  $g(s_y)$  and an “inflated” covariance matrix based on the  $\theta^{(i)'}$ . (c) Refine this procedure by using the Gaussian sampler in (b) to propose a further batch of parameters that is then adjusted via another training of the neural network. (d) Model the subset of “best” adjusted parameters via a Gaussian copula, which is then appropriately transformed to produce an approximated posterior, which is the final output of the procedure in Chen and Gutmann (2019).

Our work considers several guided samplers, including copula-based ones. There are several substantial differences with the approach proposed by Chen and Gutmann (2019). First, we do not need to introduce neural networks and the necessary tuning required for their construction. Second, at

each iteration of our sequential procedures, our guided samplers are immediately constructed from the accepted parameters and summaries obtained in the previous iteration. Third, we do not only consider Gaussian-copulas, but also Student’s t-copulas with marginal distributions which are chosen by the user instead of being learned via kernel density estimation. We explored the performance of many possible marginals: such as Gaussian, Student’s t, Gumbel, Uniform, logistic and triangular marginals.

Other contributions for sequential likelihood-free Bayesian inference, that are not within the “standard ABC” framework (i.e. procedures that are not necessarily based on specifying summary statistics that get compared via a threshold parameter  $\delta$ ), are e.g. Papamakarios and Murray (2016), Lueckmann et al. (2017), Papamakarios et al. (2019), Greenberg et al. (2019), Wiqvist et al. (2021). While these works have notable merits, we do not compare our results with theirs, as our goal is to improve the SIS-ABC and SMC-ABC samplers. In section 2, we briefly summarise sequential ABC samplers, before introducing our original proposal functions in section 3. Simulation studies are in section 4 where we consider examples with multimodal posteriors (section 4.1), highly non-Gaussian summary statistics (sections 4.1 and 4.2), large dimensional parameters (4.4), large dimensional summaries with up to 400 components (sections 4.4 and 4.5), and highly correlated posteriors (section 4.3). Finally an Appendix with theoretical results, and Supplementary Material with additional examples are provided.

## 2 Sequential ABC schemes

Throughout this section, we summarise the key features of two of the most important ABC algorithms based on sequential sampling schemes, namely SIS-ABC and SMC-ABC, since these two are at the core of our novel contributions.

### 2.1 Sequential importance sampling ABC

An obvious improvement to the basic ABC-rejection considers proposing parameters from a carefully constructed “importance sampler”  $g(\theta)$ . In this procedure, each accepted parameter receives a weight  $\pi(\theta)/g(\theta)$  to correct for the fact that the parameter was not proposed from  $\pi(\theta)$ , and the weight correction provides (weighted) samples from the corresponding approximate posterior  $\pi_\delta(\theta|s_y)$ . When  $g(\theta) \equiv \pi(\theta)$ , importance sampling ABC reduces to the ABC-rejection algorithm. Importance sampling is particularly appealing when embedded into a series of  $T$  iterations, see Algorithm 1, which can also suggest ways to construct a decreasing sequence of thresholds  $\delta_1 < \delta_2 < \dots < \delta_T$  (more on this later). This implies the introduction of  $T$  importance distributions  $g_1, \dots, g_T$ , with  $g_1(\theta) \equiv \pi(\theta)$ . The output of the algorithm provides us with weighted samples from the last iteration:  $(\theta_T^{(1)}, \tilde{w}_T^{(1)}), \dots, (\theta_T^{(N)}, \tilde{w}_T^{(N)}) \sim \pi_\delta(\theta|s_y)$ . These can be used to compute the ABC posterior mean as  $E(\theta|s) \approx \sum_{i=1}^N w_T^{(i)} \theta_T^{(i)}$  (where the  $w_t$  denote normalised weights, i.e.  $w_t^{(i)} = \tilde{w}_t^{(i)} / \sum_{j=1}^N \tilde{w}_t^{(j)}$ ) and posterior quantiles by using eq. (3.6) in Chen and Shao (1999). Otherwise, perhaps more practically, it is possible to sample  $N$  times with replacement from the set  $(\theta_T^{(1)}, \dots, \theta_T^{(N)})$ , using probabilities given by the normalised weights, and then produce histograms, or compute posterior means and quantiles by using the resampled particles (after resampling, all samples have the same normalised weight  $1/N$ ). However, Algorithm 1 does not clarify the most important issue: how to *sequentially* construct the samplers  $g_1, \dots, g_T$ . Inspired by work on sequential learning (Cappé et al., 2004, Del Moral et al., 2006), a number of sequential ABC samplers have been produced, such as Sisson et al. (2007), Toni et al. (2008), Beaumont et al. (2009), Del Moral et al. (2012). We collectively refer to these methods as SMC-ABC, as described in section 2.2.

### 2.2 Sequential Monte Carlo ABC samplers

At iteration  $t$ , SMC-ABC constructs automatically tuned proposal samplers by either considering “global” features of the collection of  $N$  accepted samples from the previous iteration  $(\theta_{t-1}^{(1)}, \tilde{w}_{t-1}^{(1)}), \dots,$

---

**Algorithm 1 Sequential importance sampling ABC (SIS-ABC)**


---

```

1: Set  $t := 1$ .
2: for  $i = 1, \dots, N$  do
3:   repeat
4:     Sample  $\theta^* \sim \pi(\theta)$ .
5:     Generate  $z^i \sim p(z|\theta^*)$  from the model.
6:     Compute summary statistic  $s^i = S(z^i)$ .
7:   until  $\|s^i - s_y\| < \delta_1$ 
8:   Set  $\theta_1^{(i)} := \theta^*$ 
9:   set  $\tilde{w}_1^{(i)} := 1$ .
10: end for
11: Obtain  $\delta_2$ .
12: for  $t = 2, \dots, T$  do
13:   for  $i = 1, \dots, N$  do
14:     repeat
15:       Sample  $\theta^* \sim g_t(\theta)$ .
16:       if  $\pi(\theta^*) = 0$  go to step 15, otherwise continue.
17:       Generate  $z^i \sim p(z|\theta^*)$  from the model.
18:       Compute summary statistic  $s^i = S(z^i)$ .
19:     until  $\|s^i - s_y\| < \delta_t$ 
20:     Set  $\theta_t^{(i)} := \theta^*$ 
21:     set  $\tilde{w}_t^{(i)} = \pi(\theta^{(i)})/g_t(\theta^{(i)})$ .
22:   end for
23:   Decrease the current  $\delta$ .
24: end for
25: Output:
26: A set of weighted parameters  $(\theta_T^{(1)}, \tilde{w}_T^{(1)}), \dots, (\theta_T^{(N)}, \tilde{w}_T^{(N)}) \sim \pi_{\delta_T}(\theta|s_y)$ .

```

---

$(\theta_{t-1}^{(N)}, \tilde{w}_{t-1}^{(N)})$ , or “local” features that are specific to each sample  $(\theta_{t-1}^{(i)}, \tilde{w}_{t-1}^{(i)})$ . In this framework, a sample is traditionally named “particle”. For example, a global feature could be the (weighted) sample covariance  $\Sigma_{t-1}$  of the particles  $(\theta_{t-1}^{(1)}, \dots, \theta_{t-1}^{(N)})$ , and this could be used in a sampler to propose particles at iteration  $t$ . More generally, if we consider the importance sampler as  $g_t(\theta) \equiv g_t(\theta|\theta_{t-1}^{(1)}, \dots, \theta_{t-1}^{(N)})$  we can set  $g_t(\theta) = q(\theta|\mu_{t-1}, \Sigma_{t-1})$ , where  $\Sigma_{t-1}$  is the previously defined covariance matrix and  $\mu_{t-1}$  is some central location of the particles at iteration  $t-1$ . A reasonable and intuitive choice is (with some abuse of notation)  $g_t(\theta) = q(\theta|\mu_{t-1}, \Sigma_{t-1}) \equiv \mathcal{N}(\mu_{t-1}, \Sigma_{t-1})$ , where  $\mathcal{N}(a, b)$  is the  $N$ -dimensional Gaussian distribution with mean  $a$  and covariance matrix  $b$ . However, this would create a global sampler that may only be appropriate if the targeted posterior is approximately Gaussian.

In the context of filtering for state-space models, a game-changer in the application of sequential importance sampling methods was the intuition in Stewart and McCarty Jr (1992) and Gordon et al. (1993) of randomly sampling a particle with replacement from the  $N$  particles with associated normalised weights  $(\theta_{t-1}^{(1)}, w_{t-1}^{(1)}), \dots, (\theta_{t-1}^{(N)}, w_{t-1}^{(N)})$ , call the sampled particle  $\theta_{t-1}^*$ , and then randomly “perturb” this to produce a  $\theta_t^{**} \sim q_t(\cdot|\theta_{t-1}^*)$  (notice the latter notation does not exclude dependence on other particles as well). For example Filippi et al. (2013) considers (among more advanced possibilities that we are going to discuss)  $\theta_t^{**} \sim \mathcal{N}(\theta_{t-1}^*, 2\Sigma_{t-1})$ . The perturbed proposal  $\theta_t^{**}$  may be accepted or not according to the usual ABC criterion. The procedure is iterated until  $N$  proposals are accepted at each iteration. The SMC-ABC algorithm is exemplified in Algorithm 2, where the key step of sampling a particle based on its weight is in step 15, and its perturbed version is in step 16. Having  $\theta_t^{**} \sim \mathcal{N}(\theta_{t-1}^*, 2\Sigma_{t-1})$  implies that the mean of the proposal sampler exploits “local” features, since perturbed draws lie within an ellipsis centred in  $\theta_{t-1}^*$ . However its covariance matrix is still global, but it is also possible to have a “local” covariance, as in the OLCM sampler below (see also Supplementary Material). In summary, an accepted particle  $\theta_t^{(i)}$  results out of (i) a randomly drawn particle from the set at iteration  $t-1$  using probabilities (normalised weights)  $\{w_{t-1}^{(i)}\}_{i=1}^N$  (ii) and an additional perturbation procedure on the particle sampled in (i). Which means that the proposal distribution for particle  $\theta^{(i)}$  is an  $N$ -components mixture distribution with mixing probabilities  $\{w_{t-1}^{(j)}\}_{j=1}^N$  and

---

**Algorithm 2 Sequential Monte Carlo ABC (SMC-ABC)**


---

```

1: Set  $t := 1$ .
2: for  $i = 1, \dots, N$  do
3:   repeat
4:     Sample  $\theta^* \sim \pi(\theta)$ .
5:     Generate  $z^i \sim p(z|\theta^*)$  from the model.
6:     Compute summary statistic  $s^i = S(z^i)$ .
7:   until  $\|s^i - s_y\| < \delta_1$ 
8:   Set  $\theta_1^{(i)} := \theta^*$ 
9:   set  $\tilde{w}_1^{(i)} := 1$ .
10: end for
11: Obtain  $\delta_2$ .
12: for  $t = 2, \dots, T$  do
13:   for  $i = 1, \dots, N$  do
14:     repeat
15:       Randomly pick (with replacement)  $\theta^*$  from the weighted set  $\{\theta_{t-1}^{(i)}, w_{t-1}^{(i)}\}_{i=1}^N$ .
16:       Perturb  $\theta^{**} \sim q_t(\cdot|\theta^*)$ .
17:       if  $\pi(\theta^{**}) = 0$  go to step 16, otherwise continue.
18:       Generate  $z^i \sim p(z|\theta^{**})$  from the model.
19:       Compute summary statistic  $s^i = S(z^i)$ .
20:     until  $\|s^i - s_y\| < \delta_t$ 
21:     Set  $\theta_t^{(i)} := \theta^{**}$ 
22:     set  $\tilde{w}_t^{(i)} = \pi(\theta_t^{(i)}) / \sum_{j=1}^N w_{t-1}^{(j)} q_t(\theta_t^{(i)}|\theta_{t-1}^{(j)})$ .
23:   end for
24:   Normalise the weights:  $w_t^{(i)} := \tilde{w}_t^{(i)} / \sum_{j=1}^N \tilde{w}_t^{(j)}$ .
25:   Decrease the current  $\delta$ .
26: end for
27: Output:
28: A set of weighted parameters  $(\theta_T^{(1)}, \tilde{w}_T^{(1)}), \dots, (\theta_T^{(N)}, \tilde{w}_T^{(N)}) \sim \pi_{\delta_T}(\theta|s_y)$ .

```

---

components  $q_t(\theta^{(i)}|\theta_{t-1}^{(j)})$  ( $j = 1, \dots, N$ ), that is  $g_t(\theta^{(i)}) = \sum_{j=1}^N w_{t-1}^{(j)} q_t(\theta_t^{(i)}|\theta_{t-1}^{(j)})$ , which motivates the importance weight

$$\tilde{w}_t^{(i)} = \pi(\theta_t^{(i)}) / \sum_{j=1}^N w_{t-1}^{(j)} q_t(\theta_t^{(i)}|\theta_{t-1}^{(j)}), \quad i = 1, \dots, N. \quad (1)$$

Notice that, in (1), the denominator has to be evaluated anew for each accepted  $\theta^{(i)}$ . One of the measures of the effectiveness of an importance or an SMC sampler is the ‘‘effective sample size’’ (ESS), where  $1 \leq \text{ESS} \leq N$ , the larger the ESS the better. At iteration  $t$ , this is traditionally approximated as  $\widehat{\text{ESS}}_t = 1 / \left( \sum_{j=1}^N (w_t^{(j)})^2 \right)$ , however alternatives are explored in Martino et al. (2017).

Some notable SMC-ABC proposal samplers are detailed in Supplementary Material. Here we briefly recall those that provide a useful comparison with our novel methods introduced in sections 3. Some of the most interesting work for the construction of such samplers is in Filippi et al. (2013). There, for the case where the interest is in constructing samplers based on perturbing a particle randomly picked from the previous iteration, they produce ways to tune the covariance matrix of Gaussian proposals that improve on Beaumont et al. (2009).

As a first approach, Filippi et al. (2013) propose the full  $\theta^{**}$  by generating at iteration  $t$  from the  $d_\theta$ -dimensional Gaussian  $q(\theta|\theta^*) \equiv \mathcal{N}(\theta^*, 2\Sigma)$ , with  $\Sigma$  being the empirical weighted covariance matrix from the particles accepted at iteration  $t - 1$ . This results in the importance weights (1) becoming (with the usual notation abuse)

$$\tilde{w}_t^{(i)} = \pi(\theta_t^{(i)}) / \sum_{j=1}^N w_{t-1}^{(j)} \mathcal{N}(\theta_t^{(i)}; \theta_{t-1}^{(j)}, 2\Sigma_{t-1}), \quad i = 1, \dots, N. \quad (2)$$

In our experiments, this proposal embedded into SMC-ABC is denoted **standard**, being in some way a baseline approach. Filippi et al. (2013) further improved on this initial approach in several ways

(details in Supplementary Material). One of these considers the “optimal local covariance matrix” (`olcm`). The key feature of this sampler is that each proposed particle  $\theta^{**}$  arises from perturbing  $\theta^*$  using a Gaussian distribution having a covariance matrix that is specific to  $\theta^*$  (hence “local”), rather than being tuned on all particles accepted at  $t - 1$  as in the `standard` sampler. To construct the `olcm` Filippi et al. (2013) define the following weighted set of particles of size  $N_0 \leq N$  at iteration  $t - 1$

$$\{\tilde{\theta}_{t-1,l}, \gamma_{t-1,l}\}_{1 \leq l \leq N_0} = \left\{ \left( \theta_{t-1}^{(i)}, \frac{w_{t-1}^{(i)}}{\bar{\gamma}_{t-1}} \right), \text{ s.t. } \|s_{t-1}^i - s_y\| < \delta_t, \quad i = 1, \dots, N \right\}, \quad (3)$$

where  $\bar{\gamma}_{t-1}$  is a normalization constant such that  $\sum_{l=1}^{N_0} \gamma_{t-1,l} = 1$ . That is, the  $N_0$  weighted particles are the subset of the  $N$  particles accepted at iteration  $t - 1$  (when using  $\delta_{t-1}$ ) having generated summaries that produce distances that are *also* smaller than  $\delta_t$ . We used the letter  $\gamma$  to denote normalised weights associated to the subset of  $N_0$  particles, rather than  $w$ , to avoid confusion. At iteration  $t$ , the `olcm` proposal is  $q_t(\theta|\theta^*) = \mathcal{N}(\theta^*, \Sigma_{\theta^*}^{\text{olcm}})$  where

$$\Sigma_{\theta^*}^{\text{olcm}} = \sum_{l=1}^{N_0} \gamma_{t-1,l} (\tilde{\theta}_{t-1,l} - \theta^*) (\tilde{\theta}_{t-1,l} - \theta^*)'.$$

Accepted particles are given unnormalised weights

$$\tilde{w}_t^{(i)} = \pi(\theta_t^{(i)}) / \sum_{j=1}^N w_{t-1}^{(j)} \mathcal{N}(\theta_t^{(i)}; \theta_{t-1}^{(j)}, \Sigma_{\theta^{(j)}}^{\text{olcm}})$$

where

$$\Sigma_{\theta^{(j)}}^{\text{olcm}} = \sum_{l=1}^{N_0} \gamma_{t-1,l} (\tilde{\theta}_{t-1,l} - \theta_{t-1}^{(j)}) (\tilde{\theta}_{t-1,l} - \theta_{t-1}^{(j)})'.$$

Evidently, we are required to store the  $N$  distances  $\|s_{t-1}^i - s_y\|$  accepted at iteration  $t - 1$ , so that it is possible to determine which indices  $i$  have distance smaller than the  $t$ -th threshold  $\delta_t$ , i.e.  $\|s_{t-1}^i - s_y\| < \delta_t$ . The computation of  $\Sigma_{\theta^*}^{\text{olcm}}$  causes some non-negligible overhead in the computations, since it has to be performed for every proposal parameter, and sanity checks on this matrix have to be performed to ensure that this is a proper covariance matrix, otherwise computer implementations will halt with an error. We postpone such discussion in section 3.2, where it is better placed, and now introduce our novel proposal samplers.

### 3 Guided sequential samplers

Here, we describe our main contributions to improve the efficiency of both SIS-ABC and SMC-ABC samplers by constructing proposal samplers that are conditional on observed summaries  $s_y$ . In a sense, our samplers “guide” the particles by using information provided by the data. As hopefully clear from section 2, samplers  $g(\theta)$  can be arbitrarily flexible. We create proposal samplers of type  $g(\theta|s_y)$  (when the entire vector parameter is proposed in block) or even conditional proposals of the type  $g(\theta_k|\theta_{-k}, s_y)$ , where  $\theta_k$  is the  $k$ -th component of a  $d_\theta$ -dimensional vector parameter  $\theta$  and  $\theta_{-k} = (\theta_1, \dots, \theta_{k-1}, \theta_{k+1}, \dots, \theta_{d_\theta})$ . The starting idea behind the construction of these samplers is loosely inspired by Picchini et al. (2022): there, a guided Gaussian proposal kernel was constructed for MCMC inference using synthetic likelihoods (Wood, 2010; Price et al., 2018). Here, we considerably extend the methodology to aid SIS-ABC and SMC-ABC, and additionally introduce non-Gaussian proposal samplers using copulas with a variety of marginal structures. To help the reader navigate the several proposals samplers we introduced in this work, we classify them in Table 1 for quick reference.

Proposal sampler	guided	family	global or local	algorithm	section
<code>standard</code>	no	Gaussian	local mean, global cov	SMC-ABC	2.2
<code>olcm</code>	no	Gaussian	local mean, local cov	SMC-ABC	2.2
<code>blocked</code>	yes	Gaussian	global mean, global cov	SIS-ABC	3.1.1
<code>blockedopt</code>	yes	Gaussian	global mean, global cov	SIS-ABC	3.1.2
<code>hybrid</code>	yes	Gaussian	global mean, global cov	SIS-ABC	3.1.3
<code>Cop-blocked</code>	yes	Gaussian or t copula	global mean, global cov	SIS-ABC	3.1.4
<code>Cop-blockedopt</code>	yes	Gaussian or t copula	global mean, global cov	SIS-ABC	3.1.4
<code>Cop-hybrid</code>	yes	Gaussian or t copula	global mean, global cov	SIS-ABC	3.1.4
<code>fullcond</code>	yes	Gaussian	local mean, global var	SMC-ABC	3.2
<code>fullcondopt</code>	yes	Gaussian	local mean, local var	SMC-ABC	3.2.1

Table 1: Proposal samplers considered in this work, categorized according to whether the sampler is guided by data or not, its distributional family, whether the sampler has features that are specific for each particle (local) or are common to all particles (global), the type of algorithm employing the proposal sampler, the relevant section introducing the sampler. All listed samplers are novel, except for `standard` and `olcm`.

### 3.1 Guided SIS-ABC samplers

In section 3.1.1, we consider a first approach for a guided Gaussian proposal function for SIS-ABC. Section 3.1.2 presents another guided Gaussian proposal function for SIS-ABC, where the covariance matrix is in some sense optimized. Finally section 3.1.4 generalizes the guided approaches for SIS-ABC to copula-based proposals.

#### 3.1.1 A first guided Gaussian SIS-ABC sampler

In Picchini et al. (2022), an MCMC proposal sampler was constructed to aid inference via synthetic likelihoods (Wood, 2010, Price et al., 2018). There, the idea was to collect the several (say  $N$ ) model-simulated summary statistics  $\{s^i\}_{i=1}^N$  that were generated at a given proposed parameter  $\theta$ , average them to obtain  $\bar{s} = \sum_{i=1}^N s^i / N$  so that, by appealing to the Central Limit Theorem, for  $N$  “large” enough,  $\bar{s}$  is approximately Gaussian distributed. Picchini et al. (2022) then observed that if the joint  $(\theta, \bar{s}^i)$  is approximately multivariate Gaussian, then a conditionally Gaussian  $g(\theta|s = s_y)$  can be constructed and used as a proposal sampler. We do not get into further detail here, as it is not necessary to motivate the construction of our samplers.

Let us now set  $d_\theta = \dim(\theta)$ ,  $d_s = \dim(s_y)$ ,  $d = d_\theta + d_s$  and denote by  $(\theta^{(i)}, s^{(i)})$  a  $d$ -dimensional particle that has been accepted at iteration  $t - 1$  of SIS-ABC. Assume for a moment that  $(\theta^{(i)}, s^{(i)})$  is a  $d$ -dimensional Gaussian distributed vector  $(\theta^{(i)}, s^{(i)}) \sim \mathcal{N}_d(m, S)$ . We stress that this assumption is made merely to construct a proposal sampler, and does not extend to the actual distribution of  $(\theta^{(i)}, s^{(i)})$ . We set a  $d$ -dimensional mean vector  $m \equiv (m_\theta, m_s)$  and the  $d \times d$  covariance matrix

$$S \equiv \begin{bmatrix} S_\theta & S_{\theta s} \\ S_{s\theta} & S_s \end{bmatrix},$$

where  $S_\theta$  is  $d_\theta \times d_\theta$ ,  $S_s$  is  $d_s \times d_s$ ,  $S_{\theta s}$  is  $d_\theta \times d_s$  and of course  $S_{s\theta} \equiv S'_{\theta s}$  is  $d_s \times d_\theta$ , where  $'$  denotes transposition. Once all  $N$  accepted particles have been collected for iteration  $t - 1$  of the SIS-ABC sampler, we estimate  $m$  and  $S$  using the accepted (weighted) particles. That is, denote with  $x_{t-1}^{(i)} := (\theta_{t-1}^{(i)}, s_{t-1}^{(i)})$  a  $d$ -dimensional particle accepted at iteration  $t - 1$ . By using their normalised weights, we have the following estimated weighted mean and weighted covariance matrix

$$\hat{m}_{t-1} = \sum_{i=1}^N w_{t-1}^{(i)} x_{t-1}^{(i)}, \quad \hat{S}_{t-1} = \frac{1}{(1 - \sum_{i=1}^N w_{t-1}^{(i)})^2} \sum_{i=1}^N w_{t-1}^{(i)} (x_{t-1}^{(i)} - \hat{m}_{t-1})(x_{t-1}^{(i)} - \hat{m}_{t-1})' \quad (4)$$

(snippets of vectorized code to efficiently compute (4) are in Supplementary Material). Once  $\hat{m}_{t-1}$  and  $\hat{S}_{t-1}$  are obtained, it is possible to extract the corresponding entries (here we disregard the “ $t - 1$ ”

iteration subscript for ease of reading)  $\hat{m}_\theta$ ,  $\hat{m}_s$  and  $\hat{S}_\theta$ ,  $\hat{S}_s$ ,  $\hat{S}_{s\theta}$ ,  $\hat{S}_{\theta s}$ . We can now use well known formulae for conditionals of a multivariate Gaussian distribution, to obtain a proposal distribution for iteration  $t$  given by  $g_t(\theta|s_y) \equiv \mathcal{N}(\hat{m}_{\theta|s_y,t-1}, \hat{S}_{\theta|s_y,t-1})$ , with

$$\hat{m}_{\theta|s_y,t-1} = \hat{m}_\theta + \hat{S}_{\theta s}(\hat{S}_s)^{-1}(s_y - \hat{m}_s) \quad (5)$$

$$\hat{S}_{\theta|s_y,t-1} = \hat{S}_\theta - \hat{S}_{\theta s}(\hat{S}_s)^{-1}\hat{S}_{s\theta}. \quad (6)$$

Hence, a parameter proposal for Algorithm 1 can be generated as  $\theta^* \sim \mathcal{N}(\hat{m}_{\theta|s_y,t-1}, \hat{S}_{\theta|s_y,t-1})$ , which has an explicit “guiding” term  $(s_y - \hat{m}_s)$ . We call  $g_t(\theta|s_y)$  a “guided SIS-ABC sampler”. To distinguish it from other guided SIS-ABC samplers we introduce later, this one is named **blocked** in our experiments, since all coordinates of  $\theta^*$  are proposed jointly, hence “in block”. Notice the guiding term  $(s_y - \hat{m}_s)$  becomes less and less relevant as  $\hat{m}_s \approx s_y$ , which is supposed to happen when  $\delta$  is small enough. Of course, a concern around the efficacy of such sampler may arise if the joint  $(\theta, s)$  is not approximately multivariate Gaussian. The case studies in sections 4.1-4.2 have markedly non-Gaussian summary statistics, however our guided sampler behaves well. However, an undesirable feature is that it may occasionally display “mode-seeking” behaviour. This means that it rapidly approaches high posterior density areas, and hence rapidly accepts promising particles in the initial iterations, but may ending up exploring mostly the area around the posterior mode, and not necessarily the tails of the targeted distribution. We address this issue in section 3.1.2 by tuning the covariance matrix of the sampler while preserving its “guided” feature.

### 3.1.2 Guided Gaussian SIS-ABC sampler with optimal local covariance

Proposal samplers can be designed according to several intuitions. For example, they could be based on the similarity with the targeted density, as suggested by a small Kullback-Leibler (KL) divergence while maximizing the acceptance probability as in Filippi et al., 2013 (see also Supplementary Material), or based on minimizing the variance of the importance weights while maximizing the acceptance probability as in Alsing et al. (2018), or using guided approaches as those outlined before. Here, we let the mean of a Gaussian sampler be the same as in equation (5), hence the proposal is guided by the observed summaries, but we construct the proposal covariance matrix following a reasoning inspired by Filippi et al. (2013). While they consider SMC-ABC and hence a perturbation  $\theta^{**}$  of a resampled particle  $\theta^*$ , in SIS-ABC we do not have such a perturbation.

For the “target” distribution denoted by  $q_{\delta_t}^*(\theta^*) = \pi_{\delta_t}(\theta^*|s_y)$ , we wish to determine a proposal  $q_{\delta_t}(\theta^*)$  by minimizing the KL divergence  $KL(q_{\delta_t}, q_{\delta_t}^*)$  between its arguments, where

$$KL(q_{\delta_t}, q_{\delta_t}^*) = \int q_{\delta_t}^*(\theta^*) \cdot \log \frac{q_{\delta_t}^*(\theta^*)}{q_{\delta_t}(\theta^*)} d\theta^*.$$

In the context of SMC-ABC, which we discuss later in section 3.2.1, Filippi et al. (2013) mention that it is possible to consider a “multi-objective optimization” problem where, in addition to minimize the KL divergence, the maximization of an “average acceptance probability” is also carried out. By transposing their reasoning in our SIS-ABC context, the multi-objective optimization is equivalent to maximizing the following  $Q$  (Filippi et al., 2013)

$$Q(q_t, \delta_t, s_y) = \int \pi_{\delta_t}(\theta^*|s_y) \log q_t(\theta^*) d\theta^* \quad (7)$$

with respect to  $q_t$ . By considering  $q_t(\theta^*) \equiv \mathcal{N}(\hat{m}_{\theta|s_y,t-1}, \Sigma_t)$  for unknown  $\Sigma_t$  and fixed  $\hat{m}_{\theta|s_y,t-1}$  defined as in (5), the resulting maximization in  $\Sigma_t$  leads to (details are in Appendix)

$$\Sigma_t = \int \pi_{\delta_t}(\theta^*|s_y) (\theta^* - \hat{m}_{\theta|s_y,t-1})' (\theta^* - \hat{m}_{\theta|s_y,t-1}) d\theta^*. \quad (8)$$

The latter integral can be approximated following the same reasoning considered for OLCM in section Supplementary Material, namely we can consider the  $N$  particles accepted at iteration  $t - 1$  (which

used a threshold  $\delta_{t-1}$ ) and select from those the  $N_0 \leq N$  particles that produced a distance  $\|s - s_y\|$  that is *also* smaller than  $\delta_t$ , to obtain

$$\hat{\Sigma}_t = \sum_{l=1}^{N_0} \gamma_{t-1,l} (\tilde{\theta}_{t-1,l} - \hat{m}_{\theta|s_y,t-1}) (\tilde{\theta}_{t-1,l} - \hat{m}_{\theta|s_y,t-1})',$$

with  $(\tilde{\theta}, \gamma)$  defined as in (3). In our experiments, we call `blockedopt` a SIS-ABC sampler (as in algorithm 1) with  $g_t(\theta|s_y) \equiv \mathcal{N}(\hat{m}_{\theta|s_y,t-1}, \hat{\Sigma}_t)$  as guided proposal. Importantly, notice that unlike `OLCM`, the covariance matrix  $\hat{\Sigma}_t$  is “global”, which means that at each iteration only one covariance matrix needs to be computed and used for all proposed particles. This relieves the computational budget from the necessity to ensure (via Cholesky decomposition and in case of numerical issues, a more expensive modified-Cholesky decomposition as in Higham, 1988) that the particle-specific covariance matrix is positive definite for each proposed particle. Of course, there is appeal in having a particle-specific “local” covariance matrix, and this is explored in section 3.2.

### 3.1.3 Hybrid guided Gaussian SIS-ABC sampler

In our experiments we consider a further type of guided Gaussian SIS-ABC sampler, which we denote `hybrid`, which is a by-product of the `blocked` and `blockedopt` strategies. At iteration  $t = 1$ , the `hybrid` sampler proposes from the prior, same as all examined strategies. At  $t = 2$ , it proposes using `blocked` for rapid convergence towards the modal area, while for  $t > 2$ , it uses `blockedopt` to correct for possible mode-seeking behaviour.

### 3.1.4 Generalised copula-based guided SIS-ABC samplers

The previously proposed guided SIS-ABC samplers assume that the proposal  $g_t(\theta|s_y)$  follows a  $d_\theta$ -dimensional Gaussian distribution with a certain mean vector  $m^*$  and covariance matrix  $S^* = (S_{ij}^*)_{i,j=1}^{d_\theta}$ . This can be generalised to make the samplers more flexible, both in terms of joint distribution and marginals. To do this, we use copulas. The idea of using copula modelling within ABC has been initially proposed by Li et al. (2017), who use a Gaussian copula for approximating the ABC posterior for a high-dimensional parameter space, and then by An et al. (2020) for modelling a high-dimensional summary statistic. Instead, we use (Gaussian and  $t$ ) copulas for the proposal sampler.

Suppose that the  $d_\theta$ -dimensional random vector  $X = (X_1, \dots, X_{d_\theta})$  has a joint cumulative distribution function  $H$  and continuous marginals  $F_1, \dots, F_{d_\theta}$ , i.e.,  $X \sim H(F_1(x_1), \dots, F_{d_\theta}(x_{d_\theta}))$ . Sklar’s theorem (Sklar, 1959) states that the joint distribution  $H$  can be rewritten in terms of  $d_\theta$  uniform marginal distributions and a multivariate copula function  $C : [0, 1]^{d_\theta} \rightarrow [0, 1]$  that describes the correlation structure between them, i.e.

$$H(x_1, \dots, x_{d_\theta}) = C(u_1, \dots, u_{d_\theta}) = C(F(x_1), \dots, F(x_{d_\theta})),$$

with  $u_j = F_j(x_j)$ ,  $j = 1, \dots, d_\theta$ . Hence, a copula is a multivariate distribution with uniform marginals. Denoting by  $h$ ,  $f_j$  and  $c$  the densities of the joint distribution  $H$ , the marginal  $F_j$  and the copula  $C$ , respectively, we have

$$h(x_1, \dots, x_{d_\theta}) = c(u_1, \dots, u_{d_\theta}) \prod_{j=1}^{d_\theta} f_j(x_j), \quad j = 1, \dots, d_\theta, \quad (9)$$

where

$$c(u_1, \dots, u_{d_\theta}) = \frac{\partial^{d_\theta}}{\partial u_1 \cdots \partial u_{d_\theta}} C(U_1, \dots, U_{d_\theta}).$$

As copula families  $C$ , we consider the Gaussian and the  $t$  copulas, corresponding on having the joint distribution  $H$  to be multivariate Gaussian and  $t$ , respectively. While the Gaussian copula is fully

characterised by a correlation matrix  $R$ , the  $t$  copulas depend on both a correlation matrix  $R$ , and the degrees of freedom  $\nu$  (cf. Appendix B), a hyperparameter which we fix, differently from Chen and Gutmann (2019), where the covariance matrix is learned via a neural network. Other copula families are available, but none of them allow for negative correlations in dimensions larger than 2, so we do not consider them. When choosing the copula and the underlying marginals, we want to preserve the mean vector  $m^*$  and the covariance matrix  $S^*$  of the guided SIS-ABC samplers. To do this, we derive the correlation matrix  $R$  from the covariance matrix  $S^*$ , and we choose the parameters of the underlying marginal distributions  $F_j$  such that  $\mathbb{E}[X_j] = m_j^*$  and  $\text{Var}(X_j) = S_{jj}^*$ . Hence, a  $d_\theta$ -dimensional parameter proposal  $\theta^* \sim g_t(\theta|s_y)$  with copula  $C$ , marginals  $F_1, \dots, F_{d_\theta}$ , mean vector  $m^*$  and covariance matrix  $S^*$  for SIS-ABC (algorithm 2) can be generated as follows:

1. Derive the parameters of the marginal distribution  $F_j$  such that  $\mathbb{E}[X_j] = m_j^*$  and  $\text{Var}(X_j) = S_{jj}^*$ ,  $j = 1, \dots, d_\theta$ .
2. Compute the correlation matrix  $R = (R_{ij})_{i,j=1}^d$  from the covariance matrix  $S^* = (S_{ij}^*)_{i,j=1}^d$ , with entries
 
$$R_{ij} = \frac{\text{Cov}(X_i, X_j)}{\sqrt{\text{Var}(X_i)\text{Var}(X_j)}} = \frac{1}{\sqrt{S_{ii}^*S_{jj}^*}}S_{ij}^*.$$
3. Simulate  $(u_1, \dots, u_{d_\theta})$  from the chosen (Gaussian or  $t$ ) copula;
4. Set  $\theta_j^* := x_j = F_j^{-1}(u_j)$ ,  $j = 1, \dots, d_\theta$  to obtain the desired parameter proposals.

Note that step 4 is well defined thanks to the marginal distributions being continuous. Finally, the proposal density needed to derive the weights of the  $i$ th particle (line 22 of Algorithm 2) can be computed via (9), using the copula densities reported in Appendix B. As underlying marginal distributions  $F_j$ , we choose the  $t$ -location scale, the logistic, the Gumbel, the Gaussian, the triangular, and the uniform distribution. The first three (resp. last two) have heavier (resp. lighter) tails than the Gaussian distribution, allowing to sample less (resp. more) around their mean values. Calculations linking the parameters of the chosen marginal distributions to the marginal mean  $m_j^*$  and variance  $S_{jj}^{2*}$  are reported in Appendix C. Note that sampling from a Gaussian copula with normal marginals corresponds to sampling from a multivariate Gaussian proposal.

### 3.2 Guided SMC-ABC samplers

Here, we wish to make the proposal function  $g_t(\cdot)$  to be more dependent on the local features of important particles from the set obtained at iteration  $t-1$ . What we mean with ‘‘local feature’’ is that we can construct proposal samplers that, similarly to standard SMC-ABC proposal samplers, may consider particle-specific samplers. More concretely, a standard choice for step 16 in Algorithm 2 is to consider  $\theta^{**} \sim \mathcal{N}(\theta^*, 2\Sigma_{t-1})$  (Beaumont et al., 2009, Filippi et al., 2013, though actually Beaumont et al., 2009 considers a diagonal covariance matrix), where the covariance matrix is common to all particles (global feature) while only the mean is particle specific (local feature). With reference to Gaussian samplers, we can construct samplers where each proposed particle at iteration  $t$  has its own specific mean and a global covariance structure and, additionally, be conditional on observed summaries  $s_y$ . Note that Filippi et al. (2013) considers also Gaussian samplers having both local means and local covariances, see e.g. the OLCM sampler, which we compare against to in our experiments. However, their approach is not obtained from a procedure that condition on  $s_y$ .

Constructing a guided and local SMC-ABC sampler is immediate, given the reasoning in section 3.1. We wish to perturb a sampled particle  $\theta^*$  to produce a proposed  $\theta^{**}$  in step 16 of Algorithm 2. Once  $\theta^*$  has been picked, we define as ‘‘augmented data’’ the vector  $(\theta^*, s_y)$  and we want to make use of such information to produce  $\theta^{**}$ . It is useful to imagine  $\theta^*$  as  $(\theta_k^*, \theta_{-k}^*)$ , if we wish to update one component at a time, using the notation established at the beginning of section 3, or as  $(\theta_{k,l}^*, \theta_{-(k,l)}^*)$  if we update a block of two components at a time, etc. In section 4.3 we consider an example where some components of  $\theta$  are highly correlated in the prior, and a sampler exploiting this fact dramatically

helps producing an efficient ABC algorithm. We illustrate the approach by focusing on perturbing a single component of  $\theta$ , as the notation is easier to convey the message, and extensions to multiple components are immediate. Therefore, here we focus on the augmented data expressed as the column vector

$$\begin{bmatrix} \theta_k^* \\ \theta_{-k}^* \\ s_y \end{bmatrix},$$

for which we assume a joint multivariate Gaussian distribution allowing us to design a ‘‘perturbation kernel’’  $q_t(\theta_k|\theta_{-k}^*, s_y)$ . Our goal is proposing for the  $k$ -th component of  $\theta$ , conditionally on the remaining  $d_\theta - 1$  coordinates of  $\theta^*$  and the whole  $s_y$ . This means that the sampler producing  $\theta_k^{**}$  does not make use of the value of  $\theta_k^*$ , but the sampler producing  $\theta_{k'}^{**}$  will make use of  $\theta_k^*$  ( $k' \neq k$ ). Under the same assumptions of joint Gaussianity considered in section 3.1, we have that  $q_t(\theta_k|\theta_{-k}^*, s_y)$  is a Gaussian sampler, which we now construct.

Say that all  $N$  accepted  $d$ -dimensional particles of type  $(\theta, s)$  have been obtained for iteration  $t-1$ . We now compute the weighted sample mean and weighed covariance matrix just as in (4), and from these we extract the following quantities

- $\hat{m}_k$ : the scalar element extracted from  $\hat{m}_{t-1}$  and corresponding to component  $k$  of  $\theta$ ;
- $\hat{S}_{k,-k}$ : the  $(d-1)$ -dimensional row vector extracted from  $\hat{S}_{t-1}$  by considering the row corresponding to  $\theta_k$  and retaining all columns except the one corresponding to  $\theta_k$ .
- $\hat{S}_{-k,-k}$ : the  $(d-1) \times (d-1)$ -dimensional matrix extracted from  $\hat{S}_{t-1}$  by eliminating the row and the column corresponding to  $\theta_k$ .
- $\begin{bmatrix} \theta_{-k}^* \\ s_y \end{bmatrix}$  the  $(d-1)$ -dimensional column vector appending  $s_y$  to the particle  $\theta_{-k}^*$ , where the latter is the  $\theta^*$  randomly picked in step 15 of Algorithm 2 with its  $k$ -th component eliminated.
- $\begin{bmatrix} \hat{m}_{-k} \\ \hat{m}_s \end{bmatrix}$  the  $(d-1)$ -dimensional column vector concatenating the  $d_\theta - 1$  (weighted) sample means of the particles for  $\theta$ , except the  $k$ -th component, and the  $d_s$  (weighted) sample means of the corresponding summary statistics.
- $\hat{\sigma}_k^2$ : the scalar value found in  $\hat{S}_{t-1}$  correspondingly to the row and column entry for  $\theta_k$ .
- $\hat{S}_{-k,k}$ : the  $(d-1)$ -dimensional column vector extracted from  $\hat{S}_{t-1}$  by retaining all rows except the one corresponding to  $\theta_k$ , and considering only the column corresponding to  $\theta_k$ .

Then, upon completion of iteration  $t-1$ , we have

$$\hat{m}_{k|s_y,t-1}^* = \hat{m}_k + \hat{S}_{k,-k}(\hat{S}_{-k,-k})^{-1} \left( \begin{bmatrix} \theta_{-k}^* \\ s_y \end{bmatrix} - \begin{bmatrix} \hat{m}_{-k} \\ \hat{m}_s \end{bmatrix} \right), \quad k = 1, \dots, d_\theta \quad (10)$$

$$\hat{\sigma}_{k|s_y,t-1}^2 = \hat{\sigma}_k^2 - \hat{S}_{k,-k}(\hat{S}_{-k,-k})^{-1} \hat{S}_{-k,k}, \quad k = 1, \dots, d_\theta. \quad (11)$$

The asterisk in  $\hat{m}_{k|s_y,t-1}^*$  is meant to emphasize that this quantity depends on the specific  $\theta^*$ , unlike the variance (11) which is common to all perturbed particles. That is in terms of its mean, the sampler has ‘‘local’’ features but global features for the covariance. We define the perturbation kernel at iteration  $t$  for component  $k$  as  $\theta_k^{**} \sim \mathcal{N}(\hat{m}_{k|s_y,t-1}^*, \hat{\sigma}_{k|s_y,t-1}^2)$ . By looping through (10)–(11) and then proposing  $\theta_k^{**} \sim \mathcal{N}(\hat{m}_{k|s_y,t-1}^*, \hat{\sigma}_{k|s_y,t-1}^2)$  for all  $k = 1, \dots, d_\theta$ , we form  $\theta^{**} = (\theta_1^{**}, \dots, \theta_{d_\theta}^{**})$ . This sampler has ‘‘local mean features’’ (its mean depends on the picked  $\theta^*$ ) but has ‘‘global’’ covariance (independent of  $\theta^*$ ), which can also be made local as described in section 3.2.1.

If we follow the procedure above, then the  $q_t(\theta|\theta^*)$  consists in the product of  $d_\theta$  1-dimensional Gaussian samplers each of type  $q_t(\theta_k|\theta_{-k}^*, s_y) = \mathcal{N}(\hat{m}_{k|s_y,t-1}^*, \hat{\sigma}_{k|s_y,t-1}^2)$ , one for each component of  $\theta$ .

While we perturb each component of  $\theta^*$  separately from the others, our approach is much different from the component-wise approach of Beaumont et al. (2009), since correlation between the dimensions of  $\theta$  is taken into account and, additionally, we condition on  $s_y$ . Once  $N$  particles  $\{\theta^{(i)}\}_{i=1}^N$  have been accepted, the importance weight (1) is given by

$$\tilde{w}_t^{(i)} = \pi(\theta_t^{(i)}) / \left\{ \sum_{j=1}^N w_{t-1}^{(j)} \prod_{k=1}^{d_\theta} \mathcal{N}(\theta_{t,k}^{(i)}; \hat{m}_{k|s_y,t-1}^{*(j)}, \hat{\sigma}_{k|s_y,t-1}^2) \right\}, \quad i = 1, \dots, N,$$

where  $\theta_{t,k}^{(i)}$  is the  $k$ -th component of the accepted  $\theta_t^{(i)}$  and  $\hat{m}_{k|s_y,t-1}^{*(j)}$  is the guided mean obtained from every sampled  $\theta^{*(j)}$  ( $j = 1, \dots, N$ )

$$\hat{m}_{k|s_y,t-1}^{*(j)} = \hat{m}_k + \hat{S}_{k,-k} (\hat{S}_{-k,-k})^{-1} \left( \begin{bmatrix} \theta_{-k}^{*(j)} \\ s_y \end{bmatrix} - \begin{bmatrix} \hat{m}_{-k} \\ \hat{m}_s \end{bmatrix} \right), \quad j = 1, \dots, N. \quad (12)$$

In our experiments, when using the SMC-ABC in algorithm 2 with guided sampler  $q_t(\theta_k | \theta_{-k}^*, s_y) = \mathcal{N}(\hat{m}_{k|s_y,t-1}^*, \hat{\sigma}_{k|s_y,t-1}^2)$ , we call the resulting procedure `fullcond` since each coordinate  $\theta_k^{**}$  is “fully conditional” on all the coordinates of  $\theta^*$  (except for  $\theta_k^*$ ). The scheme outlined is just an example, and the procedure opens up the possibility to jointly sample “blocks” of elements of  $\theta$ , conditionally on the remaining components and  $s_y$ . This turns particularly useful if it is known that some parameter components are highly correlated in the posterior, as proposing those correlated components in block can ease exploration of the posterior surface. For example, in section 4.1 we have two highly correlated parameters where proposing from  $q_t(\theta_k | \theta_{-k}^*, s_y)$  is largely suboptimal. However, in section 4.3 we exploit a-priori knowledge of the high correlation between the first two components (of a five dimensional vector  $\theta$ ), and proposing from  $q_t(\theta_1^{**}, \theta_2^{**} | \theta_{-\{1,2\}}^*, s_y)$  results in a very efficient sampler whose structure is in Supplementary Material.

Similarly to the guided SIS-ABC `blocked` sampler, the SMC-ABC `fullcond` sampler we have just constructed may suffer from “mode seeking” problems. In the next section, we address this issue and construct a version that uses an “optimal local” covariance matrix.

### 3.2.1 Guided SMC-ABC samplers with optimal local covariance

We now follow a similar route to that pursued in section 3.1.2 when “optimizing” the covariance matrix of a guided SIS-ABC sampler, but we now focus on the SMC-ABC `fullcond` case. At iteration  $t$ , denote by  $\theta^{**}$  the perturbed version of some  $\theta^*$  obtained from the particles accepted at  $t-1$  according to  $\theta^{**} \sim q_t(\cdot | \theta^*)$ . We can imagine accepting the couple  $(\theta^{**}, \theta^*)$  (even though of course we are only interested in  $\theta^{**}$ ) if and only if  $\|s^{**} - s_y\| < \delta_t$ , where  $s^{**} \sim p(s | \theta^{**})$ . A joint proposal distribution for  $(\theta^{**}, \theta^*)$  should somehow resemble the target product distribution induced by sampling  $\theta^{**}$  and  $\theta^*$  independently from  $\pi_{\delta_t}(\theta | s_y)$  and  $\pi_{\delta_{t-1}}(\theta | s_y)$ , respectively, and whose density is  $\pi_{\delta_t}(\theta | s_y) \cdot \pi_{\delta_{t-1}}(\theta | s_y)$ .

The approach detailed in Filippi et al. (2013) considers the “target product” distribution denoted by  $q_{\delta_{t-1}, \delta_t}^*(\theta^*, \theta^{**}) = \pi_{\delta_t}(\theta^{**} | s_y) \cdot \pi_{\delta_{t-1}}(\theta^* | s_y)$  and determines a proposal  $q_{\delta_{t-1}, \delta_t}(\theta^*, \theta^{**})$  by minimizing the KL divergence  $KL(q_{\delta_{t-1}, \delta_t}, q_{\delta_{t-1}, \delta_t}^*)$  between its arguments, where

$$KL(q_{\delta_{t-1}, \delta_t}, q_{\delta_{t-1}, \delta_t}^*) = \int q_{\delta_{t-1}, \delta_t}^*(\theta^*, \theta^{**}) \cdot \log \frac{q_{\delta_{t-1}, \delta_t}^*(\theta^*, \theta^{**})}{q_{\delta_{t-1}, \delta_t}(\theta^*, \theta^{**})} d\theta^* d\theta^{**}.$$

This time the multi-objective criterion to optimize is equivalent to maximizing the following  $Q$  with respect to  $q_t$

$$Q(q_t, \delta_{t-1}, \delta_t, s_y) = \int \pi_{\delta_t}(\theta^{**} | s_y) \cdot \pi_{\delta_{t-1}}(\theta^* | s_y) \log q_t(\theta^{**} | \theta^*) d\theta^* d\theta^{**}. \quad (13)$$

The above is useful if we want to obtain a proposal sampler that has “global properties”, that is a sampler that is not specific for a given  $\theta^*$ , and in fact the latter is considered as a variable in the

integrands for both the KL and the  $Q$  quantities above, so that both the KL and  $Q$  result independent of  $\theta^*$  (and  $\theta^{**}$ ) since it is integrated out.

We now build on the reasoning above to detail how to optimize with respect to  $q_t$  in the context of our guided SMC-ABC sampler outlined in section 3.2. The sampler  $q_t$  we are interested in optimizing is a univariate Gaussian with mean  $\hat{m}_{k|s_y,t-1}^*$  given by equation (10). There, the particle  $\theta^*$  enters as  $\theta_{-k}^*$  and is considered *fixed* rather than a variable as in (13). That is, we want to obtain a sampler that is optimal “locally” for  $\theta^*$ , and optimize  $q_t$  with respect to an unknown variance that is specific to the sampled  $\theta^*$ , rather than being global for all particles. In this case, the KL criterion is simplified as  $\theta^*$  is not a variable, and we have

$$Q(q_t, \delta_t, s_y) = \int \pi_{\delta_t}(\theta^{**}|s_y) \log q_t(\theta^{**}|\theta^*) d\theta^{**},$$

where in our case  $q_t(\theta^{**}|\theta^*, s_y) \equiv \prod_{k=1}^{d_\theta} \mathcal{N}(\hat{m}_{k|s_y,t-1}^*, \sigma_k^{*2})$  and the  $\sigma_k^*$  are unknowns we wish to maximize  $Q$  for. Note that the  $\sigma_k^*$  refers to a specific  $\theta^*$ , hence the asterisk. By equating the first derivative of  $Q$  with respect to a generic  $\sigma_k^*$  to zero, we have that (see details in Appendix)

$$\sigma_k^{*2} = \int \pi_{\delta_t}(\theta_k^{**}|s_y) (\theta_k^{**} - \hat{m}_{k|s_y,t-1}^*)^2 d\theta_k^{**}. \quad (14)$$

The latter can be approximated via standard Monte Carlo. In fact, even though we only have  $N$  samples obtained at iteration  $t-1$  (and not at iteration  $t$  since these have not been sampled yet), we can use the same argument as for the OLCM criterion. That is, from the  $N$  particles sampled and accepted at iteration  $t-1$  using  $\delta_{t-1}$ , we subselect the  $N_0$  particles that generated distances that happen to be also smaller than  $\delta_t$ , denoted  $\tilde{\theta}_{t-1,l}$  with normalised weights  $\gamma_{t-1,l}$ . These  $N_0$  particles are therefore sampled from  $\pi_{\delta_t}(\theta_k|s_y)$ , and we can approximate  $\sigma_k^{*2}$  with

$$\hat{\sigma}_k^{*2} = \sum_{l=1}^{N_0} \gamma_{t-1,l} (\tilde{\theta}_{t-1,k,l} - \hat{m}_{k|s_y,t-1}^*)^2, \quad k = 1, \dots, d_\theta$$

with  $\tilde{\theta}_{t-1,k,l}$  the  $k$ -th component of  $\tilde{\theta}_{t-1,l}$ . Therefore, we have constructed a guided SMC-ABC sampler having “local” features for both the mean and the variance, since they both depend on  $\theta^*$  (unlike `fullcond` in section 3.2 where the mean is local but the variance is global). At iteration  $t$ , this samples from (with the usual abuse of notation)  $q_t(\theta^{**}|\theta^*, s_y) \equiv \prod_{k=1}^{d_\theta} \mathcal{N}(\hat{m}_{k|s_y,t-1}^*, \hat{\sigma}_k^{*2})$ , and therefore

$$\tilde{w}_t^{(i)} = \pi(\theta_t^{(i)}) / \left\{ \sum_{j=1}^N w_{t-1}^{(j)} \prod_{k=1}^{d_\theta} \mathcal{N}(\theta_{t,k}^{(i)}; \hat{m}_{k|s_y,t-1}^{*(j)}, \hat{\sigma}_k^{*(j)2}) \right\}, \quad i = 1, \dots, N$$

where  $\hat{m}_{k|s_y,t-1}^{*(j)}$  is as in (12) and

$$\hat{\sigma}_k^{*(j)2} = \sum_{l=1}^{N_0} \gamma_{t-1,l} (\tilde{\theta}_{t-1,k,l} - \hat{m}_{k|s_y,t-1}^{*(j)})^2, \quad j = 1, \dots, N, \quad k = 1, \dots, d_\theta.$$

In our experiments, we call `fullcondopt` the sampler just outlined. An exciting display of a particular version of this sampler is in section 4.3 where two components  $(\theta_1, \theta_2)$  of a 5-dimensional parameter  $\theta$  are highly correlated in the prior, and this fact is exploited with great success by the sampler. Details on this specific sampler are in Supplementary Material.

## 4 Examples

In this section, we consider several experiments to assess the performances of our guided proposals (cf. Section 3) against those of the non-guided `standard` and `olcm` proposal samplers (cf. Section

2.2). We refer to Table 1 for an outline/classification of the proposal samplers considered here. The `cop-blocked`, `cop-blockedopt` and `cop-hybrid` approaches use either Gaussian or t copulas, with triangular, generalised t, logistic, Gumbel, uniform or normal marginal distributions. As the samplers based on the Gumbel marginal distributions perform poorly across the different examples, we only report them in the first case study as an illustration. In Sections 4.1 and 4.2, we compare the algorithms at prefixed  $\delta$  values over ten independent estimation runs for each method. In particular, we focus on the quality of the posterior inference, the median acceptance rates (with first and third quartiles) and the running (wallclock) times. In Sections 4.3 and 4.5, we also consider the online updating of  $\delta$ . When we use the online updating strategy, this is performed as follows:  $\delta_t$  is taken as a percentile of all the ABC distances  $\rho_{t-1} = \|s(z) - s_y\|$  produced at iteration  $t-1$  (including those from rejected proposals), say the  $\psi$ -th percentile. However, occasionally, this may not be enough to produce monotonously decreasing  $\delta$ 's: we therefore impose the following: call  $\tilde{\delta}_t$  the  $\psi$ -th percentile of  $\rho_{t-1}$ . Then, we take  $\delta_t := \tilde{\delta}_t$  if  $\tilde{\delta}_t < \delta_{t-1}$ , otherwise we set  $\delta_t := 0.95\delta_{t-1}$ .

## 4.1 Two-moons with bimodal posterior and non-Gaussian summaries

As some of the novel proposal samplers are multivariate Gaussian distributions, derived by exploiting multivariate Gaussianity of the pair  $(\theta, s)$  as in section 3.1.1, it is of interest to check their performance when such assumption is not met. For this reason, here we consider the *two-moons model*, a bimodal two-dimensional model characterised by highly non-Gaussian summary statistics (cf. Supplementary material) and a crescent-shaped posterior (under some parameter setting). We consider the same setup as in Greenberg et al. (2019) and Wiquist et al. (2021) for simulation-based inference. The output of the two-moons model is a two-dimensional vector  $z \in \mathbb{R}^2$  generated via

$$\begin{aligned} a &\sim U(-\pi/2, \pi/2) \\ r &\sim \mathcal{N}(0.1, 0.01^2) \\ p &= (r \cos(a) + 0.25, r \sin(a)) \\ z &= p + \left( -\frac{|\theta_1 + \theta_2|}{\sqrt{2}}, \frac{-\theta_1 + \theta_2}{\sqrt{2}} \right), \end{aligned}$$

see the supplementary material in Greenberg et al. (2019) for further discussion. Here, we take priors  $\theta_j \sim U(-1, 1)$  ( $j = 1, 2$ ), assume observed data  $y_{\text{obs}} = (0, 0)$  and consider the identity function as summary statistics function, i.e.  $S(z) = z$  and thus the data themselves. We fix the number of particles to  $N = 1000$ , and produce ten independent estimation runs for each method, comparing them at eleven prefixed  $\delta_t$  values, namely  $\delta_t \in \{4, 3, 2, 1, 0.5, 0.4, 0.3, 0.2, 0.1, 0.08, 0.06\}$ .

As exact posterior inference via MCMC is possible, we use it as a benchmark. First, we obtain 1,000 MCMC posterior draws via the Python simulator<sup>1</sup> associated to Lueckmann et al. (2021). Then, we compute the order-1 Wasserstein distances (Sommerfeld and Munk, 2018) between each of the ABC and the MCMC posteriors using the R package `transport` (Schuhmacher et al., 2020). The results of the medians of the log-Wasserstein distances are reported in Figure 1 (the quartiles are not shown to ease the reading of the plot, but the variability across the 10 runs is very small). Interestingly, the guided `blocked` and `copula-blocked` approaches have the smallest Wasserstein distances during the first five iterations, that is when approaching the high-posterior probability region. At smaller values of  $\delta_t$ , when more precise local information is needed, the methods perform similarly, except at the smallest  $\delta_t$ , where the non-guided `standard` and `olcm` display slightly larger distances. The different types of copulas and marginal distributions yield similar results, except for the Gumbel distribution, which performs poorly in all iterations across all copula-based samplers, yielding particles sampled from the ABC posterior covering only a small sub-region of one of the two moons, as illustrated in Figure 2 for one run of the `Gaussian-Cop-blocked`. The `Gaussian-Cop-blocked` (and `t-Cop-blocked`, figure not shown) with uniform marginals performed similarly bad in most of the runs, with particles covering a

<sup>1</sup>The Python code is available at [https://github.com/sbi-benchmark/sbibm/tree/main/sbibm/tasks/two\\_moons](https://github.com/sbi-benchmark/sbibm/tree/main/sbibm/tasks/two_moons)

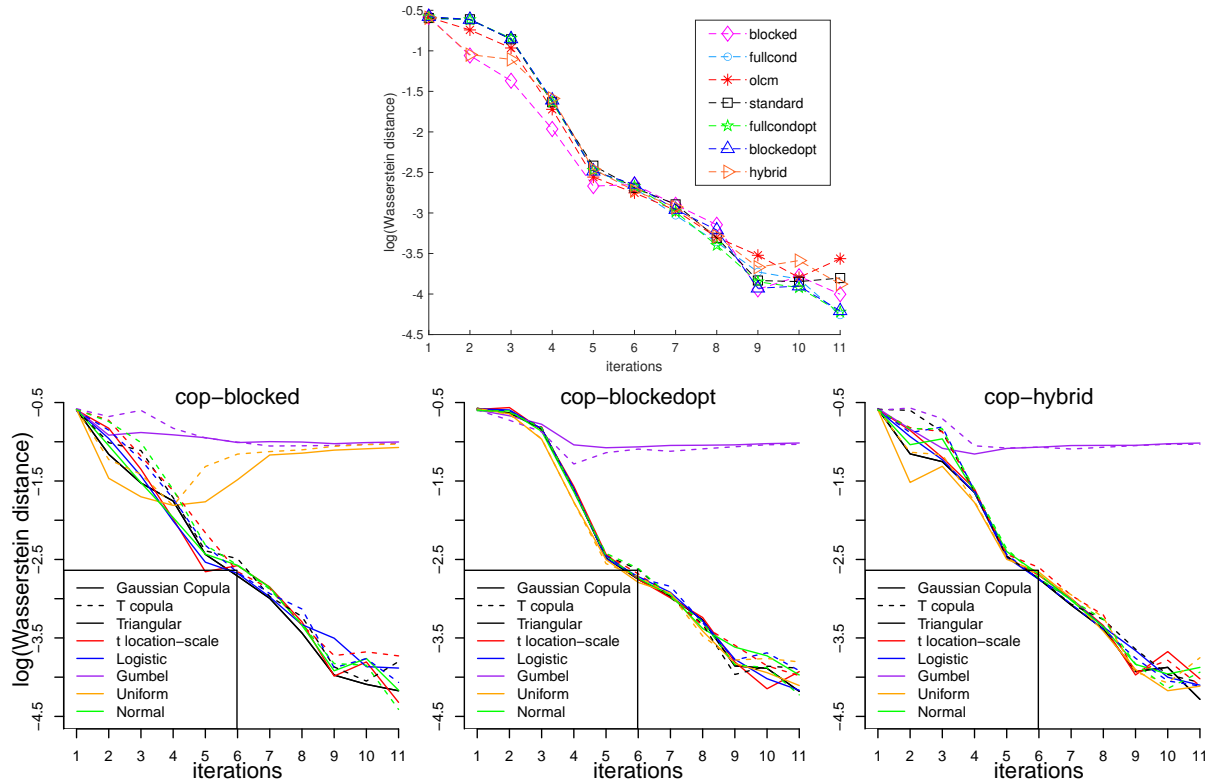


Figure 1: Two-moons model: median log-Wasserstein distances between the the “exact”(MCMC) posterior and ABC posteriors obtained via the guided or non-guided samplers, across ten independent estimations. Top: non-copula-based methods (both guided and non-guided). Bottom: copula-based guided **blocked** (left), **blockedopt** (center), **hybrid** (right).

sub-region of only one of the two moons (see Figure 2, first run) and both moons only in few attempts (see Figure 2, ninth run).

Median acceptance rates (and first and third quartiles) are reported in Figure 3, and appear very stable across the ten runs, except for **cop-blocked** with uniform marginals, where the performance varies with the run. As also observed in Filippi et al. (2013), **olcm** is superior to **standard** in terms of acceptance rate, but both are outperformed across all iterations by all our novel guided methods except **fullcondopt**. Note that the differences between the acceptance rates are large in early iterations, which is where the samples are still very dispersed in the posterior surface, and we thus we want to spend the least time possible to rule out the initial “bad” particles, which is especially relevant for models that are computationally intensive to simulate. When we consider the wallclock running times, Figure 4 reveals that **olcm** requires way more time than any guided method to accept a particle (which can be well-invested time if the final inference is improved), and the guided **fullcond**, **block**, **blockedopt** and **hybrid** methods are the fastest in accepting particles. Overall, on our desktop machine (Intel Core i7-7700 CPU 3.60GHz 32 GB RAM) and without using any parallelization, the full simulation consisting of all ten runs was completed in 5.5 minutes (with **blocked**), 5.4 minutes (**blockedopt**), 5.7 minutes (**hybrid**), 4.8 minutes (**fullcond**), 17.7 minutes (**fullcondopt**), 38.7 minutes (**olcm**) and 23.6 (20.8) minutes (**standard**). These are major time-differences given that the toy model is particularly simple to simulate. Copula methods are intrinsically slower in simulating proposals due to the more complicated construction of a generic copula sampler and the less optimized numerical libraries compared to libraries implementing multivariate Gaussian samplers, independently on whether

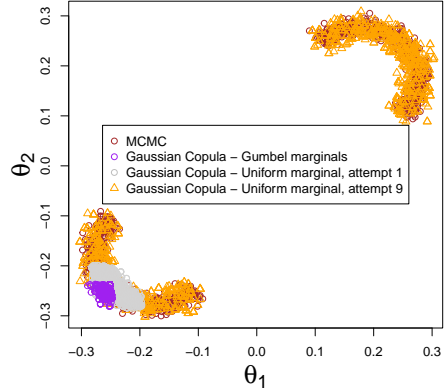


Figure 2: Two-moons model: 1,000 MCMC draws from the exact posterior (brown) and from the ABC posteriors obtained using the `Gaussian-cop-blocked` sampler with Gumbel marginals (purple) and uniform marginals from run 1 (grey) and 9 (orange). The ABC draws obtained from copulas with uniform marginals cover the whole true posterior region only in some runs (here run number 9), targeting a small sub-region of one of the two moons in most of the cases (here the first run), while those from the Gumbel marginals cover an even smaller sub-region in all runs.

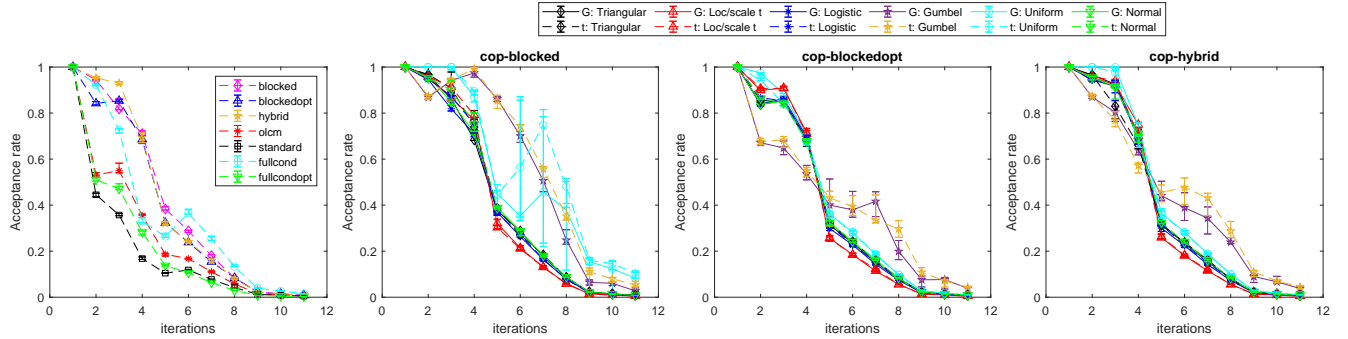


Figure 3: Two-moons model: median acceptance rates and error bars with first and third quartile across ten independent runs at each iteration. (Left panel) Non-copula based methods, both guided and not-guided; (center-left) `cop-blocked`; (center-right) `cop-blockedopt`, (right) `cop-hybrid`. The copula-based methods are derived using either Gaussian (G) or t copulas for different marginals, as described in the legend.

the codes are run in, say, R or Matlab (e.g. the `Gaussian-cop-blocked`, `Gaussian-cop-blockedopt` and `Gaussian-cop-hybrid` with normal marginals take 8.1, 11.4 and 9.4 minutes, instead of 5.5, 5.4 and 5.7 minutes of the corresponding `blocked`, `blockedopt` and `hybrid`. Since the acceptance rates of the guided-copula samplers are similar to those of the proposed Gaussian samplers, the wallclock times of the guided-copula samplers will become lower than the alternative non-guided samplers should the implementation of the R/Matlab copula built-in routines be improved (which is outside the scope of this work).

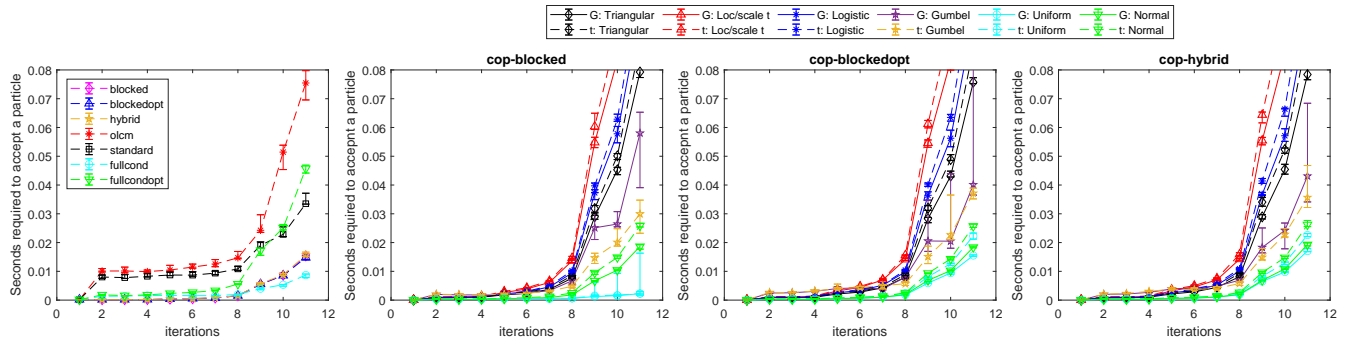


Figure 4: Two-moons model: median acceptance rates for the number of seconds required to accept a particle and error bars with first and third quartile, across ten independent runs at each iteration. (Left panel) Non-copula based methods, both guided and not-guided; (center-left) `cop-blocked`, (center-right) `cop-blockedopt`, (right) `cop-hybrid`. The copula-based methods are derived using either Gaussian (G) or t copulas for different marginals, as described in the legend.

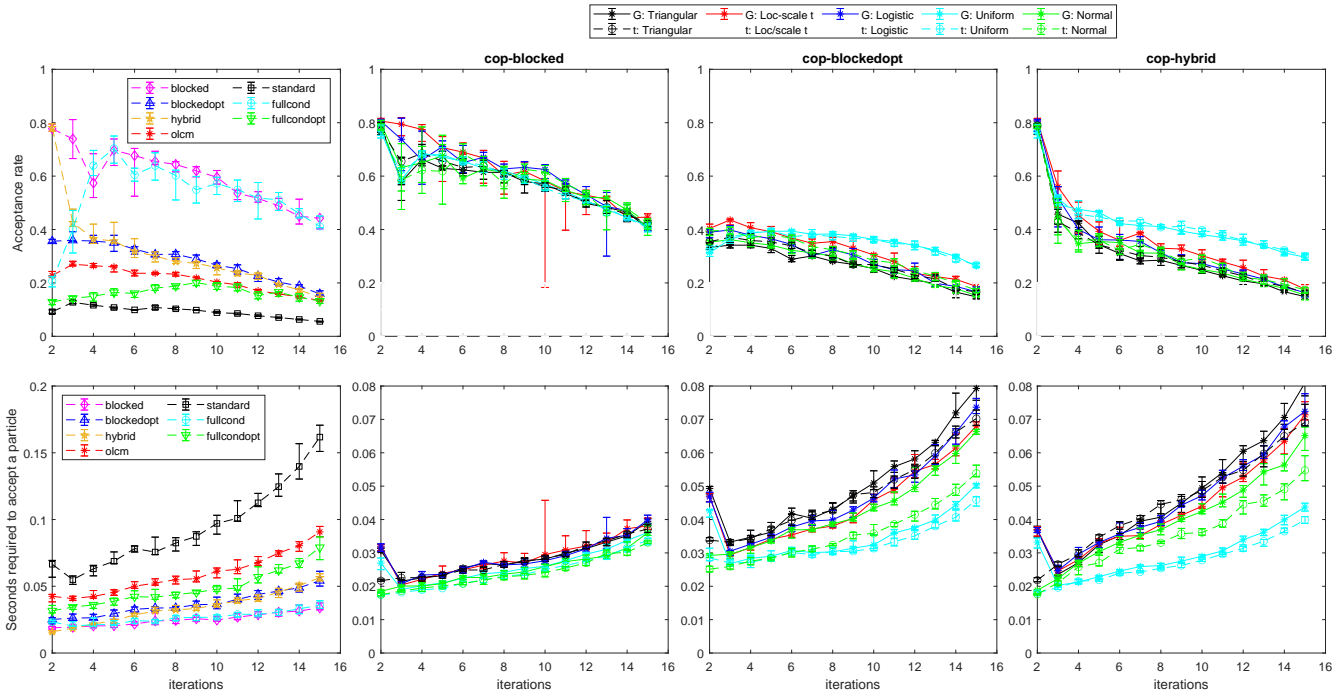


Figure 5: Boom-and-bust model: median acceptance rates and error bars with first and third quartile (top figures) and number of seconds required to accept a particle (bottom figures) across ten independent runs. (Left panel) Non-copula based methods both guided and not-guided, `cop-blocked` (center-left), `cop-blockedopt` (center-right), `cop-hybrid` (right). The copula-based methods are derived using either Gaussian (G) or t copulas for different marginals, as described in the legend. Note: we had to choose different scales of the y-axes for comparing the number of seconds required to accept a particle for the non-copula vs copula-based methods, in order to make the latter more readable.

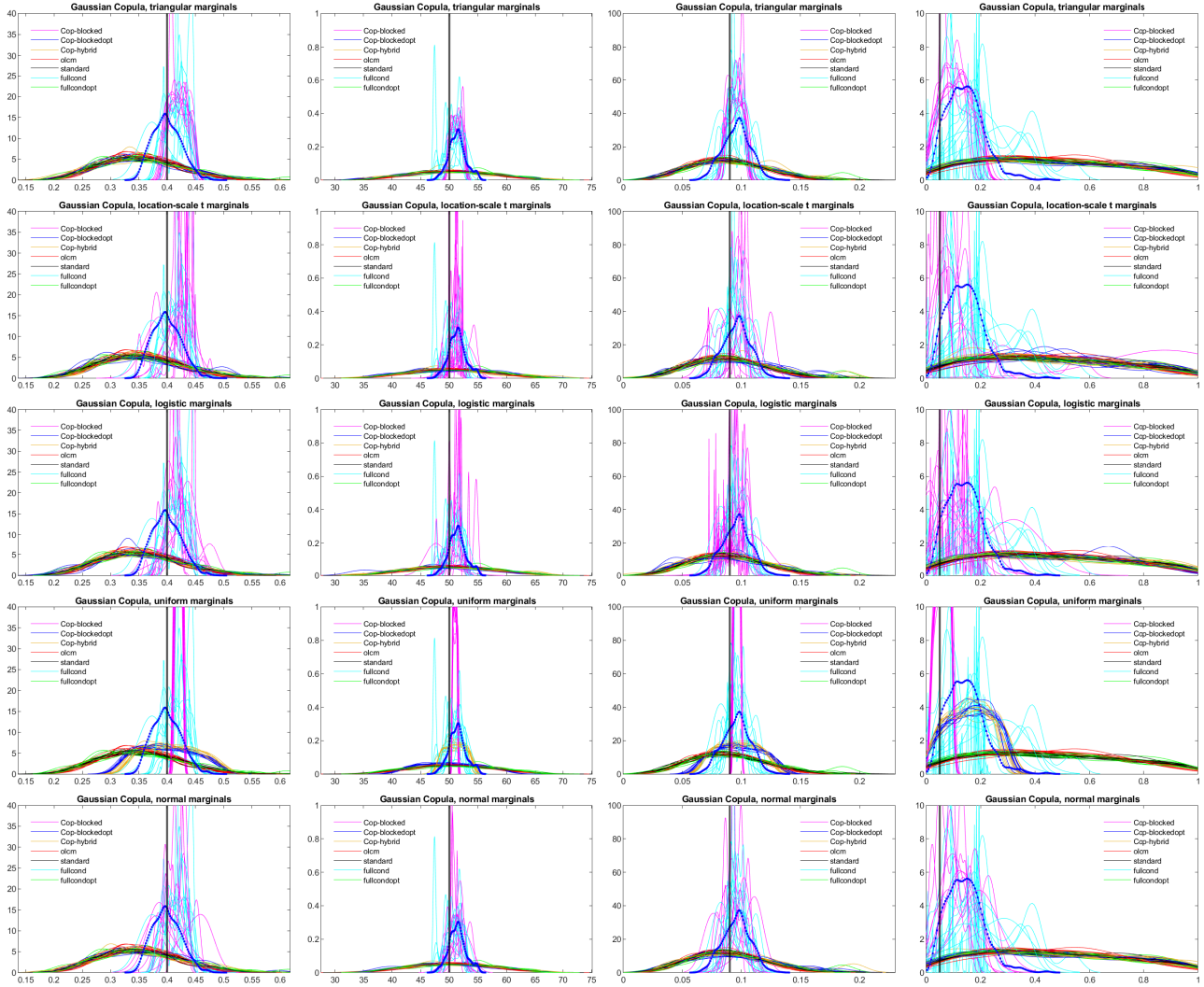


Figure 6: Boom-and-bust model: marginal posterior densities at the last iteration in all ten estimation runs obtained with all methods and Gaussian copulas with all considered marginals. True parameters value are denoted by the vertical dot-dashed lines. Robust semiBSL (blue); copula-blocked (magenta); copula-blockedopt (gray); copula-hybrid (orange); olcm (red); standard (black); fullcond (cyan); fullcondopt (green). Remember that copula-blocked (magenta), copula-blockedopt (gray), copula-hybrid (orange) with Gaussian copula and Gaussian marginals correspond to blocked, blockedopt and hybrid, respectively.

## 4.2 Recruitment boom-and-bust with highly skewed summaries

We now challenge our guided proposals samplers, constructed assuming joint normality of the particle pairs  $(\theta, s)$ , on another example characterised by highly non-Gaussian summary statistics. Such example was also considered in Fasiolo et al. (2018), An et al. (2020) and Picchini et al. (2022) in the context of synthetic likelihood, to test how that methodology, constructed under approximately Gaussian distributed summary statistics, performed. The *recruitment boom-and-bust model* is a stochastic

discrete time model  $(N_t)_{t \in \mathbb{N}}$  that can be used to describe the fluctuation of population sizes over time. Given the population size  $N_t$  and parameter  $\theta = (r, \kappa, \alpha, \beta)$ , with  $r > 0$ ,  $\kappa > 0$ ,  $\beta > 0$ ,  $\alpha \in (0, 1)$ , the population size  $N_{t+1}$  at time  $t + 1$  follows the following distribution

$$N_{t+1} \sim \begin{cases} \text{Poisson}(N_t(1+r)) + \epsilon_t, & \text{if } N_t \leq \kappa \\ \text{Binom}(N_t, \alpha) + \epsilon_t, & \text{if } N_t > \kappa \end{cases},$$

where  $\epsilon_t \sim \text{Pois}(\beta)$  is a stochastic term. The population oscillates between high and low sizes for several cycles. Same as in An et al. (2020) and Picchini et al. (2022), true parameters are set to  $r = 0.4$ ,  $\kappa = 50$ ,  $\alpha = 0.09$  and  $\beta = 0.05$  and we assume a fixed and known initial size  $N_1 = 10$ . The chosen value of  $\beta$  gives rise to highly non-Gaussian summaries, as illustrated in the Supplementary Material. We have the same modelling and data generation setup as in the previously cited references: the priors are set to  $r \sim U(0, 1)$ ,  $\kappa \sim U(10, 80)$ ,  $\alpha \sim U(0, 1)$ ,  $\beta \sim U(0, 1)$ , and to generate a dataset we first simulate values for the  $(N_t)$  process for 300 steps, then we discard the first 50 values. Therefore, the used data are the remaining 250 values. For a dataset  $y$ , we define differences and ratios as  $\text{diff}_y = \{y_i - y_{i-1}; i = 2, \dots, 250\}$  and  $\text{ratio}_y = \{(y_i + 1)/(y_{i-1} + 1); i = 2, \dots, 250\}$ , respectively. We then consider the sample mean, variance, skewness and kurtosis of  $y$ ,  $\text{diff}_y$  and  $\text{ratio}_y$  as our summary statistic, for a total of twelve summaries.

Same as for the two-moons example, here we produce comparisons between methods based on pre-fixed values for  $\delta_t$ . In particular, we use tolerances  $(\delta_1, \dots, \delta_{15}) = (3.5, 3, 2.8, 2.6, 2.4, 2.2, 2.1, 2, 1.9, 1.8, 1.7, 1.6, 1.5, 1.4, 1.3)$  and always consider  $N = 1,000$  particles. In all experiments, before starting any ABC algorithm, we first collect 5,000 simulated summaries produced from the prior predictive distribution, and then compute the mean-absolute-deviation (MAD) of each of the twelve-dimensional simulated summaries, which we use to standardise the difference between observed and simulated summaries, i.e. the ABC distances are  $(\sum_{j=1}^{12} ((s_j^* - s_{y,i})/\text{MAD}_j)^2)^{1/2}$ . The ABC posteriors for ten independent runs, obtained with different methods, are reported in Figure 6. As the true posterior is unavailable, and since ABC is notoriously underperforming when the size of the summaries is larger than a handful, here we consider the posterior obtained via the robustified semiparametric Bayesian synthetic likelihood (semiBSL) of An et al. (2020) as reference. This is because (i) BSL (Price et al., 2018) can better handle summaries having large dimension, and (ii) compared to BSL, semiBSL has been shown to be more robust to departures from Gaussianity, as it is the case here (the highly non-Gaussian distribution of the summaries is reported in Supplementary Material).

We run semiBSL for 3,000 MCMC iterations using 200 model simulations at each proposed parameter and we then disregard the first 1,000 iterations as burn-in. Compared to semiBSL, inference via ABC is expected to return wider marginals due to the nonparametric nature of ABC and the ‘‘curse of dimensionality’’ when the summaries’ dimension increases. This does not happen for **blocked**, **copula-blocked** and **fullcond** (see Figure 6 and the Figure for the copula-based samplers with t copula in the Supplementary). However, this is because both **blocked**, its copula variant, and **fullcond** can be ‘‘mode-seeking’’, that is they may overly explore the region around the mode, neglecting the tails, which motivated the creation of the ‘‘optimized versions’’ **blockedopt** and **fullcondopt**, as described in sections 3.1.2 and 3.2.1, respectively. However, the issue is less evident when choosing **cop-blocked** with triangular marginals as sampler (with either Gaussian or t copulas), which benefits from having a wider support than the uniform distribution (which is too ‘‘overconfident’’) and a higher probability of sampling within three standard deviations from the mean compared to other marginals, see Figure 10 in Appendix C. Something interesting happens for **cop-blocked** and **cop-hybrid** with uniform marginals. While the former yields the most peaked ABC posterior marginals, the latter leads to ABC posteriors which are closer to those of the semiBSL than the other methods, benefiting from the mode-seeking behavior at iteration one (coming from **cop-blocked**) followed by **cop-blockedopt**. All other methods have posteriors that are wider than those from semiBSL, as expected, and are also more consistent across the multiple independent runs, which is due to higher ESS values, as observed in a figure in the Supplementary Material. Note that narrower ABC posteriors could be obtained by further reducing  $\delta$ , incurring in a higher computational cost though. Guided approaches show

higher acceptance rates and are also faster in terms of runtime compared to the considered traditional approaches. This can be observed in Figure 5, where the medians, the first and third quartiles of the acceptance rates (top panels) and the number of seconds required to accept a particles (bottom panels) are reported. While we find that the guided `blocked`, `cop-blocked` and `fullcond` are uniformly the best ones in terms of both higher acceptance rate and lower runtimes, we should not forget that this is a consequence of the “mode seeking” behaviour of these methods, and the optimized `blockedopt` (and its by-product `hybrid`) and `fullcondopt` may generally be preferred. The locally optimal guided `fullcondopt` and non-guided `olcm` have similar acceptance rates for small values of  $\delta$ , with the latter being slower than the former. Finally, `standard` has the lowest acceptance rate, yielding then the largest runtime. Unlike for the two-moon case study, not only the wallclock times of the guided-samplers based on copulas are comparable to their corresponding Gaussian variants, but `cop-blockedopt` and `cop-hybrid` with uniform marginals yield higher acceptance rates and smaller runtimes than `blockedopt` and `hybrid`, respectively, see Figure 5, third and fourth column.

### 4.3 Twisted prior with an highly correlated posterior

We now consider a model with a challenging posterior characterised by a strong correlation between some of the parameters. This case study is particularly interesting, as the likelihood only provides location information about the unknown parameter, while the dependence structure in the posterior comes mostly from the prior, so the posterior dependence changes direction depending on whether the likelihood locates the posterior in the left or right tail of the prior (see Nott et al. (2018) for a graphical illustration). This case study was analysed in an ABC context in Li et al. (2017). The model assumes observations  $y = (y_1, \dots, y_{d_\theta})$  drawn from a  $d_\theta$ -dimensional Gaussian  $y \sim \mathcal{N}(\theta, \Psi)$ , with  $\theta = (\theta_1, \dots, \theta_{d_\theta})$  and diagonal covariance matrix  $\Psi = \text{diag}(\sigma_0, \dots, \sigma_0)$ . The prior is the “twisted-normal” prior of Haario et al. (1999), with density function proportional to

$$\pi(\theta) \propto \exp \left\{ -\frac{\theta_1^2}{200} - \frac{(\theta_2 - b\theta_1^2 + 100b)^2}{2} - \mathbb{1}_{\{d_\theta > 2\}} \sum_{j=3}^{d_\theta} \theta_j^2 \right\},$$

where  $\mathbb{1}_B$  denotes the indicator function of the set  $B$ . This prior is essentially a product of independent Gaussian distributions with the exception that the component for  $(\theta_1, \theta_2)$  is modified to produce a “banana shape”, with the strength of the bivariate dependence determined by the parameter  $b$ . Simulation from  $\pi(\theta)$  is achieved by first drawing  $\theta$  from a  $d_\theta$ -dimensional multivariate Gaussian as  $\theta \sim \mathcal{N}(0, A)$ , where  $A = \text{diag}(100, 1, \dots, 1)$ , and then placing the value  $\theta_2 + b\theta_1^2 - 100b$  in the slot for  $\theta_2$ . We consider a value for  $b$  that induces a strong correlation in the prior between the first two components of  $\theta$ . Specifically, we use the same setup as Li et al. (2017), namely  $\sigma_0 = 1$ ,  $b = 0.1$  and  $d_\theta = 5$ , i.e. both  $y_{\text{obs}}$  and  $\theta$  have length five, with observations given by the vector  $y_{\text{obs}} = (10, 0, 0, 0, 0)$ . We take the identity function as summary statistic, that is  $s = S(y) = y$ . We use  $N = 1,000$  particles, set an initial  $\delta_1 = 50$  and let  $\delta_t$  automatically decrease across iterations by taking  $\psi = 1$  (first percentile of the distances), as described at the beginning of Section 4, until the updated  $\delta$  value gets smaller than 0.25, when the inference is then stopped. This is then independently repeated for ten times on the same data for each method.

The log-Wasserstein distances between the “exact” posterior (approximated with 1,000 posterior samples obtained via MCMC) and the ABC approximations for the ten estimation runs are reported in Figure 7. To exploit the a-priori knowledge of the strong correlation between  $(\theta_1, \theta_2)$ , we consider here a version of `fullcondopt` (which we call `fullcondoptblocked`) that proposes jointly a perturbed  $(\theta_1^{**}, \theta_2^{**})$  conditionally on the  $(\theta_3^*, \theta_4^*, \theta_5^*)$  from the previous iteration, while the remaining coordinates are perturbed one-by-one conditionally on all the others as  $q(\theta_k^{**} | \theta_{-k}^*, s_y)$  ( $k = 3, 4, 5$ ), (see the Supplementary Material for the details of this sampler). What we notice is that the non-guided `olcm` reaches small log-Wasserstein distances after 15 iterations, but then continues for a few more iterations to approach  $\delta = 0.25$  (Panel A in Figure 7). The non-guided `standard` not only requires even more iterations, but also ultimately does not return distances as small as `olcm` (Panel A). The guided

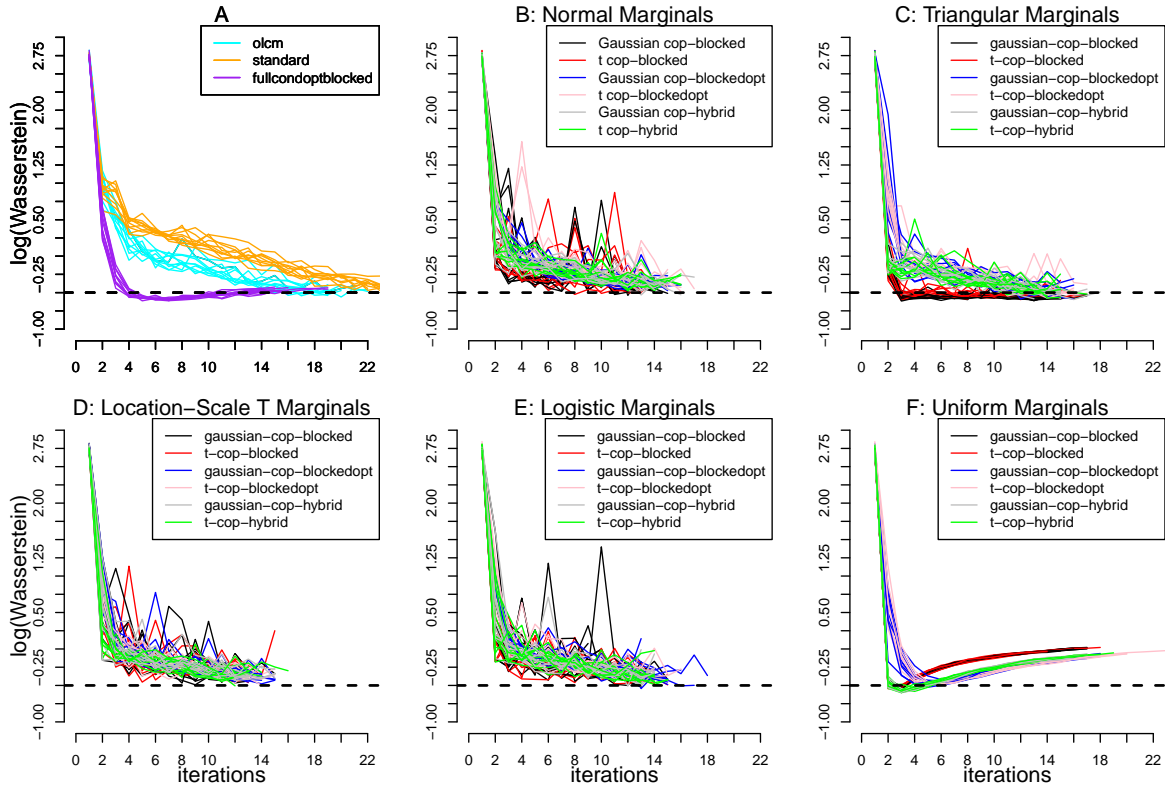


Figure 7: Twisted model: Wasserstein log-distances with respect to the true posterior for ten independent runs. Panel A: `olcm` (red), `standard` (black) and `fullcondopt` with  $(\theta_1, \theta_2)$  blocked (green). Panels B-F: `cop-blocked`, `cop-blockedopt`, `cop-hybrid` for both Gaussian and t copulas and normal (B), triangular (C), location-scale t (D), logistic (E) and uniform (F) marginals. The dashed line marks a log-distance value of -0.5 (an arbitrary value only meant to ease eye-comparisons). Some runs are shorter than others depending on how many iterations it took to reach a value of  $\delta$  smaller than 0.25.

`fullcondoptblocked` (Panel A) and all guided SIS-ABC methods (Panels B-F), either based on copulas or not, stop earlier than the non-guided methods, and have log-Wasserstein distances lower than those of `olcm` at the first few iterations and then becomes similar, except for the `cop-blocked` with triangular marginals, whose log-Wasserstein distances are smaller than `olcm` across all iterations. However, even when the distances are similar, those from the guided-samplers are obtained more rapidly thanks to a higher acceptance rate and a lower total wallclock time, see Supplementary Material. In particular, in the second iteration the guided methods display a 4-to-6 times larger acceptance rate compared to non-guided ones (in the first iteration all samplers are equivalent since proposals are generated from the prior). The second iteration is a particularly critical one for the computational budget, since particles are typically scattered far from the bulk of the true posterior. Low values of the ESS are responsible for a larger variability between different runs, as in this case only few particles are resampled at the last iteration, and these appear to differ between runs. With larger ESS, the number of particles contributing to the several posteriors is higher, thus producing posteriors that are more similar between runs. Among all copula-based guided SIS-ABC, the results of `cop-blocked` with triangular marginals (Panel C) or the guided-copula ABC-SIS with uniform marginals (Panel F) are less sensible to variability across independent runs, as the guided SMC-ABC `fullcondoptblocked` (Panel A). However, the distances obtained from marginal uniforms increase with the iterations, as the consequence of the method becoming somehow overconfident, see the Supplementary Material,

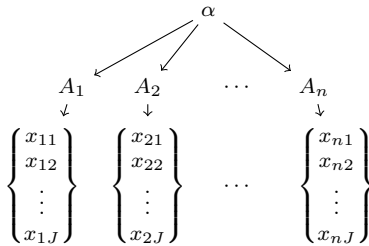


Figure 8: The hierarchical g-and-k model.

where the contour plots of the ABC posteriors at the last iteration of  $(\theta_1, \theta_2)$  are reported. Something similar happens also to `fullcondoptblocked`. Deriving a “sanity check” to prevent this deterioration in the inference performance, while of interest, is out of the scope of this work. However, a possible suggestion would be to stop the methods once the acceptance rate becomes lower than 1.5% for two consecutive iterations (similarly to Del Moral et al., 2012), indicating that it is unlikely that inference will be improved at an additional computational cost. Among all methods, we recommend using `cop-blocked` with triangular marginals, as it has the merit of being robust across several runs and, more importantly, having small log-Wasserstein distances starting from as few as three iterations.

#### 4.4 Hierarchical g-and-k model with high-dimensional summaries

We now consider a high-dimensional model from Clarté et al. (2021). This is a hierarchical version of the g-and-k model, with the latter being often used as a toy case-study in simulation-based inference (e.g. Fearnhead and Prangle, 2012). The g-and-k distribution is used to model non-standard data through five parameters  $\theta = (A, B, g, k, c)$ , though in practice  $c$  is often fixed to 0.8 (Prangle, 2017), as we do here (and thus  $\theta = (A, B, g, k)$ ). The g-and-k distribution is defined by its quantile function  $F^{-1}(z; \theta)$ , where  $F^{-1}(z; \theta) : [0, 1] \rightarrow \mathbb{R}$  is given by

$$F^{-1}(z; \theta) = A + B \left[ 1 + c \frac{1 - \exp(-g \cdot r(z))}{1 + \exp(-g \cdot r(z))} \right] (1 + r^2(z))^k r(z), \quad (15)$$

where  $r(z)$  is the  $z$ th standard normal quantile,  $A \in \mathbb{R}$  and  $B > 0$  are location and scale parameters, respectively, and  $g \in \mathbb{R}$  and  $k > -0.5$  are related to the distribution’s skewness and kurtosis, respectively. An evaluation of (15) returns a draw ( $z$ th quantile) from the g-and-k distribution. Alternatively, a single scalar draw from the g-and-k distribution can be easily simulated by tossing a standard Gaussian draw  $r^* \sim \mathcal{N}(0, 1)$  and then plugging it in place of  $r(z)$  in (15). Same as Clarté et al. (2021), we assume to have observations  $x_{ij}$  ( $i = 1, \dots, n, j = 1, \dots, J$ ) from a hierarchical g-and-k model, where each  $J$ -dimensional vector  $x_i = (x_{i1}, \dots, x_{iJ})$  is characterised by its own parameter  $A_i$ , while  $(B, g, k)$  are common to all  $n$  units, and are assumed known. We assume  $A_i \sim \mathcal{N}(\alpha, 1)$  for  $\alpha$  unknown, and  $x_{ij} \sim gk(A_i, B, g, k)$ , see Figure 8. We also assume  $\alpha \sim \text{Unif}(-10, 10)$ , and infer the parameter vector  $\theta = (\alpha, A_1, \dots, A_n)$ . Here, we generate data with  $n = 20$ ,  $J = 1,000$  by using  $(B, g, k, \alpha) = (0.192, 0.622, 0.438, 5.707)$ . Same as Clarté et al. (2021), summary statistics for  $x_i$  are the vector of nine quantiles  $\text{quant}(x_i, l/8)$  ( $l = 0, 1, \dots, 8$ ) where  $\text{quant}(x, p)$  is the  $p$ -th quantile of sample  $x$ . This setting leads to a challenging inference problem for ABC, as the vector  $\theta$  to infer is 21-dimensional, and summary statistics are a vector of length  $9n = 180$ .

An exact posterior is not available here, so we compare  $N = 10^4$  draws sampled from the considered particle-based methods, in particular `olcm`, `standard`, `hybrid` and `cop-hybrid`, with  $N$  posterior samples from the ABC-Gibbs sampler of Clarté et al. (2021), which is suited for hierarchical models<sup>2</sup>. We set an initial  $\delta_1 = 50$  and let  $\delta_i$  automatically decrease across iterations as described at the beginning of section 4 by taking  $\psi = 5$  (fifth percentile of all simulated distances), stopping the

<sup>2</sup>We appropriately modified the code at <https://github.com/GClarte/ABCG> to work with our data and model settings.

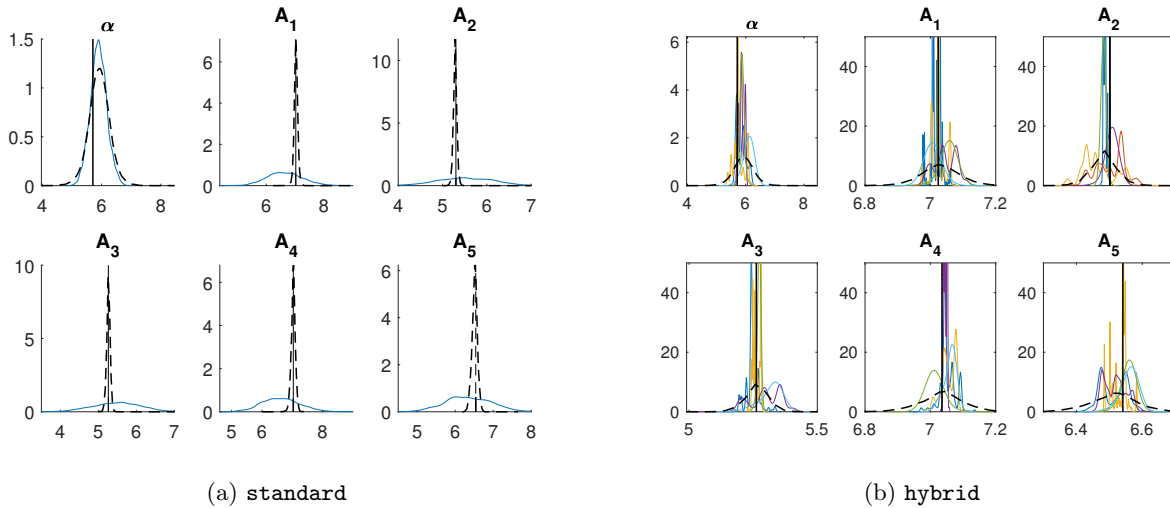


Figure 9: Hierarchical g-and-k: posteriors displayed only for  $(\alpha, A_1, \dots, A_5)$ , using: (a) **standard** at iteration  $t = 26$  and  $\delta = 2.14$  after  $14.5 \cdot 10^6$  model simulations; (b) five inference runs of **hybrid** all reaching  $\delta = 0.62$ , using for each run around  $10^6$  model simulations. Dashed lines are posteriors from ABC-Gibbs. Black vertical lines mark ground-truth values.

methods as soon as the updated  $\delta$  value gets smaller than 0.62. However, not all methods manage to reach this value in reasonable time. In terms of running times, **standard** was very slow, meaning that for a *single* run with 14.5 million model simulations, the threshold was still around  $\delta = 2.14$  at iteration  $t = 26$ . The non-guided **standard** resulted in quite uninformative marginal posteriors for the  $A_i$  parameters, see Figure 9 (for ease of display, we only report inference for  $\alpha$  and  $A_1, \dots, A_5$ ). Hence, not much is being learned except for  $\alpha$ , despite the large number of simulations. On the contrary, with **hybrid**, we locate the true parameters with high precision. In each of the runs, **hybrid** reached  $\delta = 0.62$  with an effort between  $9 \cdot 10^5$  and  $10^6$  model simulations, depending on the run, hence a speedup of *at least* fourteen times compared to **standard**, and likely to be much larger than this, given that we do not know for how much longer **standard** should run to reach satisfying inference. Notice that for this experiment the guided **hybrid** is plagued by a very small ESS, implying that posterior variability is different between runs. However, ultimately, the bulk of the posteriors from the **hybrid** sampler appears similar to that from the ABC-Gibbs method. With **olcm**, results appear more encouraging than **standard** (shown in Supplementary Material). However, if we consider inference after 1 million model simulations (same as **hybrid**), the posterior corresponds to  $\delta = 1.87$  and hence is still fairly spread. Moreover, it took about 55 hours with **olcm** to reach  $\delta = 0.70$ , compared to about 6 minutes with **hybrid** to reach  $\delta = 0.62$ . This opens up for the possibility to run multiple instances in parallel of **hybrid** (or other guided methods), given the high speed of this method, so to rapidly collect many posterior draws that can counteract the low ESS. Another possibility may be to incorporate guided proposal samplers into the SMC-ABC of Del Moral et al. (2012), which is designed to progressively, albeit slowly, reduce  $\delta$  while maintaining a reasonably high ESS value.

#### 4.5 Cell motility and proliferation with high-dimensional summaries

Finally, we consider a simulation study that was presented in Price et al. (2018) in the context of comparing ABC methods and synthetic likelihoods. This case study is interesting for us since the vector of summary statistics is high dimensional and therefore supposedly challenging for ABC (we initially consider the case where  $s_y$  has 145 components and then up to 289 and even 433). The study is reported in Supplementary Material and the main take away is that SMC-based strategies are able to

deal with such large dimensionality, unlike the ABC-MCMC reported in Price et al. (2018). Moreover, for this example, we found that the Bayesian synthetic likelihood method of Price et al. (2018) (the original version, we did not try more recent developments), which is an MCMC sampler, was unable to mix even for parameters set exactly at ground truth values when increasing the summaries size to 289. With guided and non-guided SMC-ABC instead, we managed to perform inference using summaries with up to dimension 433.

## 5 Discussion

We have introduced a range of proposal samplers to accelerate inference when using sequential ABC methods, notably sequential importance sampling (SIS-ABC) and sequential Monte Carlo (SMC-ABC). The acceleration is implied by the construction of proposal samplers that are made conditional to the summary statistics of the data, such that the proposed draws rapidly converge to the bulk of the posterior distribution. Because of this conditioning, we called our proposal samplers “guided”. As an example, in a challenging case study (hierarchical g-and-k model, Section 4.4) customary non-guided SMC-ABC samplers require many hours to approach a gold-standard ABC posterior obtained with the ad-hoc (for hierarchical models) ABC-Gibbs of Clarté et al. (2021), while our methods require about 6 minutes. We introduced a variety of guided copula-based proposal samplers (both Gaussian and t-distributed, with six considered distributions of the marginals of the copula), as well as guided multivariate Gaussian proposals. The copula-based samplers are general and flexible. Among them, those based on Gaussian copulas may be preferred, yielding higher ESS and being slightly faster than the  $t$  copulas, while yielding similar performance. Overall, the best copula-based sampler is the `cop-blocked` with triangular marginal distributions, followed by the `cop-hybrid` with uniform marginals. However, copula-based samplers involve more operations to produce a proposal compared to multivariate Gaussian samplers: this difference is tenuous if the model simulator is expensive, since in this case the computational bottleneck is the forward model simulation. However, if the model is particularly simple (as in some of our toy-models such as two-moons), then copula-based samplers result slower to run than sampling from multivariate Gaussians. This is not a disadvantage if the geometry of the posterior is such that the copula-model better adapts to its exploration, as it happens for the twisted model (in the case of `cop-blocked` with triangular marginals. As a comparison with our methods, we considered the most commonly implemented proposal sampler, which in fact we named `standard`, which is the one from Beaumont et al. (2009) and Filippi et al. (2013) (found in all the most used ABC software packages and papers considering SMC-ABC), and the sampler called OLCM in Filippi et al. (2013). We have challenged our methods by considering posteriors with multimodal surfaces (two-moons), highly non-Gaussian summary statistics (two-moons and recruitment boom-and-bust), high dimensional parameter space (hierarchical g-and-k), high dimensional summaries with more than hundreds components (hierarchical g-and-k and cell motility model), and highly correlated posteriors (twisted model). In all these experiments, on the one hand, our methods obtained satisfying ABC inference. On the other hand, they did so more rapidly than the non-guided proposal samplers, sometimes way more rapidly (two-moons, hierarchical g-and-k and twisted prior).

All our novel samplers collect, at each iteration, the accepted summaries and reuse those to create our guided proposal samplers. As such, we found that it is best to not allow the initial threshold  $\delta_1$  to be too large, as this would too liberally accept summary statistics that are extremely different from observations. This would allow the inclusion of extremely poor realizations from the forward model to contribute to the covariance matrices of the summary statistics, thus resulting in a poor initial sampler.

Our guided proposals are easy to construct and are immediately computed based on accepted parameters and summary statistics, not introducing thus any substantial overhead. For example, there is no need to construct and train a deep neural network (unlike in the guided method of Chen and Gutmann, 2019). We believe that the simplicity, and effectiveness, of our proposal samplers makes them appealing and easy to incorporate into the user’s toolbox.

## Acknowledgments

UP acknowledges support from the Swedish Research Council (Vetenskapsrådet 2019-03924) and the Chalmers AI Research Centre (CHAIR).

## References

- J. Alsing, B. D. Wandelt, and S. M. Feeney. Optimal proposals for approximate Bayesian computation. [arXiv preprint arXiv:1808.06040](#), 2018.
- Z. An, L. F. South, D. J. Nott, and C. C. Drovandi. Accelerating Bayesian synthetic likelihood with the graphical lasso. *Journal of Computational and Graphical Statistics*, 28(2):471–475, 2019.
- Z. An, D. J. Nott, and C. Drovandi. Robust bayesian synthetic likelihood via a semi-parametric approach. *Statistics and Computing*, 30:543–557, 2020.
- M. A. Beaumont, W. Zhang, and D. J. Balding. Approximate Bayesian computation in population genetics. *Genetics*, 162(4):2025–2035, 2002.
- M. A. Beaumont, J.-M. Cornuet, J.-M. Marin, and C. P. Robert. Adaptive approximate bayesian computation. *Biometrika*, 96(4):983–990, 2009.
- M. G. Blum and O. François. Non-linear regression models for approximate bayesian computation. *Statistics and computing*, 20(1):63–73, 2010.
- L. Bornn, N. S. Pillai, A. Smith, and D. Woodard. The use of a single pseudo-sample in approximate Bayesian computation. *Statistics and Computing*, 27(3):583–590, 2017.
- O. Cappé, A. Guillin, J.-M. Marin, and C. P. Robert. Population monte carlo. *Journal of Computational and Graphical Statistics*, 13(4):907–929, 2004.
- M.-H. Chen and Q.-M. Shao. Monte Carlo estimation of Bayesian credible and HPD intervals. *Journal of Computational and Graphical Statistics*, 8(1):69–92, 1999.
- Y. Chen and M. U. Gutmann. Adaptive gaussian copula abc. In *The 22nd International Conference on Artificial Intelligence and Statistics*, pages 1584–1592. PMLR, 2019.
- G. Clarté, C. P. Robert, R. J. Ryder, and J. Stoehr. Componentwise approximate bayesian computation via gibbs-like steps. *Biometrika*, 108(3):591–607, 2021.
- P. Del Moral, A. Doucet, and A. Jasra. Sequential monte carlo samplers. *Journal of the Royal Statistical Society: Series B (Statistical Methodology)*, 68(3):411–436, 2006.
- P. Del Moral, A. Doucet, and A. Jasra. An adaptive sequential monte carlo method for approximate bayesian computation. *Statistics and computing*, 22(5):1009–1020, 2012.
- R. Dutta, M. Schoengens, L. Pacchiardi, A. Ummadisingu, N. Widmer, J.-P. Onnela, and A. Mira. ABCpy: A high-performance computing perspective to approximate bayesian computation. [arXiv preprint arXiv:1711.04694](#), 2017.
- R. G. Everitt. Bootstrapped synthetic likelihood. [arXiv preprint arXiv:1711.05825](#), 2017.
- Y. Fan and S. Sisson. *Handbook of approximate Bayesian computation*, chapter ABC samplers. Chapman and Hall/CRC, 2018. also available as [arXiv:1802.09650](#).
- M. Fasiolo, S. N. Wood, F. Hartig, M. V. Bravington, et al. An extended empirical saddlepoint approximation for intractable likelihoods. *Electronic Journal of Statistics*, 12(1):1544–1578, 2018.

- P. Fearnhead and D. Prangle. Constructing summary statistics for approximate Bayesian computation: semi-automatic approximate Bayesian computation. Journal of the Royal Statistical Society: Series B (Statistical Methodology), 74(3):419–474, 2012.
- S. Filippi, C. P. Barnes, J. Cornebise, and M. P. Stumpf. On optimality of kernels for approximate Bayesian computation using sequential Monte Carlo. Statistical applications in genetics and molecular biology, 12(1):87–107, 2013.
- N. J. Gordon, D. J. Salmond, and A. F. Smith. Novel approach to nonlinear/non-Gaussian bayesian state estimation. In IEE proceedings F (radar and signal processing), volume 140, pages 107–113. IET, 1993.
- D. Greenberg, M. Nonnenmacher, and J. Macke. Automatic posterior transformation for likelihood-free inference. In International Conference on Machine Learning, pages 2404–2414. PMLR, 2019.
- H. Haario, E. Saksman, and J. Tamminen. Adaptive proposal distribution for random walk Metropolis algorithm. Computational Statistics, 14(3):375–395, 1999.
- N. J. Higham. Computing a nearest symmetric positive semidefinite matrix. Linear algebra and its applications, 103:103–118, 1988.
- J. Li, D. J. Nott, Y. Fan, and S. A. Sisson. Extending approximate Bayesian computation methods to high dimensions via a Gaussian copula model. Computational Statistics & Data Analysis, 106: 77–89, 2017.
- J.-M. Lueckmann, P. J. Goncalves, G. Bassetto, K. Öcal, M. Nonnenmacher, and J. H. Macke. Flexible statistical inference for mechanistic models of neural dynamics. arXiv preprint arXiv:1711.01861, 2017.
- J.-M. Lueckmann, J. Boelts, D. S. Greenberg, P. J. Gonçalves, and J. H. Macke. Benchmarking simulation-based inference. arXiv preprint arXiv:2101.04653, 2021.
- P. Marjoram, J. Molitor, V. Plagnol, and S. Tavaré. Markov chain Monte Carlo without likelihoods. Proceedings of the National Academy of Sciences, 100(26):15324–15328, 2003.
- L. Martino, V. Elvira, and F. Louzada. Effective sample size for importance sampling based on discrepancy measures. Signal Processing, 131:386–401, 2017.
- D. J. Nott, V. M.-H. Ong, Y. Fan, and S. Sisson. High-dimensional abc. arXiv:1802.09725, 2018.
- G. Papamakarios and I. Murray. Fast  $\varepsilon$ -free inference of simulation models with bayesian conditional density estimation. In Advances in neural information processing systems, pages 1028–1036, 2016.
- G. Papamakarios, D. Sterratt, and I. Murray. Sequential neural likelihood: Fast likelihood-free inference with autoregressive flows. In The 22nd International Conference on Artificial Intelligence and Statistics, pages 837–848. PMLR, 2019.
- U. Picchini, U. Simola, and J. Corander. Sequentially guided MCMC proposals for synthetic likelihoods and correlated synthetic likelihoods. Bayesian Analysis, 2022. doi: 10.1214/22-BA1305.
- D. Prangle. gk: An R package for the g-and-k and generalised g-and-h distributions. arXiv:1706.06889, 2017.
- L. F. Price, C. C. Drovandi, A. Lee, and D. J. Nott. Bayesian synthetic likelihood. Journal of Computational and Graphical Statistics, 27(1):1–11, 2018.
- J. W. Priddle, S. A. Sisson, D. T. Frazier, I. Turner, and C. Drovandi. Efficient Bayesian synthetic likelihood with whitening transformations. Journal of Computational and Graphical Statistics, 2021. doi: 10.1080/10618600.2021.1979012.

- J. K. Pritchard, M. T. Seielstad, A. Perez-Lezaun, and M. W. Feldman. Population growth of human y chromosomes: a study of y chromosome microsatellites. *Molecular biology and evolution*, 16(12): 1791–1798, 1999.
- D. Schuhmacher, B. Bähre, C. Gottschlich, V. Hartmann, F. Heinemann, and B. Schmitzer. *transport: Computation of Optimal Transport Plans and Wasserstein Distances*, 2020. URL <https://cran.r-project.org/package=transport>. R package version 0.12-2.
- Y. Schälte, E. Klinger, E. Alamoudi, and J. Hasenauer. pyabc: Efficient and robust easy-to-use approximate bayesian computation. *arXiv preprint arXiv:2203.13043*, 2022.
- S. A. Sisson and Y. Fan. *Handbook of Markov chain Monte Carlo*, chapter Likelihood-free MCMC. Chapman & Hall/CRC, New York., 2011.
- S. A. Sisson, Y. Fan, and M. M. Tanaka. Sequential monte carlo without likelihoods. *Proceedings of the National Academy of Sciences*, 104(6):1760–1765, 2007.
- S. A. Sisson, Y. Fan, and M. Beaumont. *Handbook of Approximate Bayesian Computation*. Chapman and Hall/CRC, 2018.
- M. Sklar. Fonctions de répartition à n dimensions et leurs marges. *Inst. Stat. Univ. Paris*, 8:229–231, 1959.
- M. Sommerfeld and A. Munk. Inference for empirical wasserstein distances on finite spaces. *Journal of the Royal Statistical Society: Series B (Statistical Methodology)*, 80(1):219–238, 2018.
- L. Stewart and P. McCarty Jr. Use of Bayesian belief networks to fuse continuous and discrete information for target recognition, tracking, and situation assessment. In *Signal Processing, Sensor Fusion, and Target Recognition*, volume 1699, pages 177–185. International Society for Optics and Photonics, 1992.
- T. Toni, D. Welch, N. Strelkowa, A. Ipsen, and M. P. Stumpf. Approximate bayesian computation scheme for parameter inference and model selection in dynamical systems. *Journal of the Royal Society Interface*, 6(31):187–202, 2008.
- R. D. Wilkinson. Approximate bayesian computation (abc) gives exact results under the assumption of model error. *Statistical applications in genetics and molecular biology*, 12(2):129–141, 2013.
- S. Wiqvist, J. Frelsen, and U. Picchini. Sequential neural posterior and likelihood approximation. *arXiv preprint arXiv:2102.06522*, 2021.
- S. N. Wood. Statistical inference for noisy nonlinear ecological dynamic systems. *Nature*, 466(7310): 1102–1104, 2010.

## A Appendix A

Here we first detail the derivation of (8), and afterwards we consider the derivation of (14). By considering  $q_t(\theta^*) \equiv \mathcal{N}(\hat{m}_{\theta|s_y,t-1}, \Sigma_t)$  for unknown  $\Sigma_t$  and fixed  $\hat{m}_{\theta|s_y,t-1}$  defined as in (5), we have that

$$Q(q_t, \delta_t, s_y) = \int \pi_{\delta_t}(\theta^* | s_y) \left( -\frac{d_{\theta}}{2} \log(2\pi) - \frac{1}{2} \log |\Sigma_t| - \frac{1}{2} (\theta^* - \hat{m}_{\theta|s_y,t-1})' \Sigma_t^{-1} (\theta^* - \hat{m}_{\theta|s_y,t-1}) \right) d\theta^*. \quad (16)$$

To maximize  $Q$  with respect to  $q_t$  (i.e. with respect to  $\Sigma_t$ ), we can disregard several terms in (16) that do not depend on  $\Sigma_t$ , by also noting that  $\int \pi_{\delta_t}(\theta^*|s_y)d\theta^* = 1$ , and obtain

$$\begin{aligned} Q(q_t, \delta_t, s_y) &\propto -\frac{1}{2} \log |\Sigma_t| - \frac{1}{2} \int \pi_{\delta_t}(\theta^*|s_y)(\theta^* - \hat{m}_{\theta|s_y, t-1})' \Sigma_t^{-1} (\theta^* - \hat{m}_{\theta|s_y, t-1}) d\theta^* \\ &= \frac{1}{2} \log |\Sigma_t^{-1}| - \frac{1}{2} \int \pi_{\delta_t}(\theta^*|s_y)(\theta^* - \hat{m}_{\theta|s_y, t-1})' \Sigma_t^{-1} (\theta^* - \hat{m}_{\theta|s_y, t-1}) d\theta^*, \end{aligned}$$

where in the latter equality we have used that for a squared matrix  $A$ ,  $|A^{-1}| = |A|^{-1}$ . Now consider a symmetric matrix  $M$  and define  $\Sigma_t = M^{-1}$ . In order to find the optimal  $\Sigma_t$ , maximizing  $Q$  is equivalent to maximizing the real-valued function  $g(M)$  with respect to  $M$ , where

$$g(M) = \log |M| - \int \pi_{\delta_t}(\theta^*|s_y)(\theta^* - \hat{m}_{\theta|s_y, t-1})' M (\theta^* - \hat{m}_{\theta|s_y, t-1}) d\theta^*.$$

The resulting maximization leads to (8).

As for the derivation of (14), by getting rid of terms not depending on any  $\sigma_k^*$ , we have that  $Q$  is proportional to

$$\begin{aligned} Q(q_t, \delta_t, s_y) &\propto - \int \pi_{\delta_t}(\theta^{**}|s_y) \left( \sum_{k=1}^{d_\theta} \log \sigma_k^* + \sum_{k=1}^{d_\theta} \frac{(\theta_k^{**} - \hat{m}_{k|s_y, t-1}^*)^2}{2\sigma_k^{*2}} \right) d\theta_1^{**} \cdots d\theta_{d_\theta}^{**} \\ &= - \sum_{k=1}^{d_\theta} \log \sigma_k^* - \frac{1}{2\sigma_k^{*2}} \int \pi_{\delta_t}(\theta^{**}|s_y) \sum_{k=1}^{d_\theta} (\theta_k^{**} - \hat{m}_{k|s_y, t-1}^*)^2 d\theta_1^{**} \cdots d\theta_{d_\theta}^{**}. \end{aligned}$$

By setting equal to zero the first derivative of  $Q$  with respect to a generic  $\sigma_k^*$ , we get (14).

## B Appendix B

Here, we report the copula functions  $C(u_1, \dots, u_{d_\theta})$  and the copula densities  $c(u_1, \dots, u_{d_\theta})$  of the Gaussian and t copulas. Let  $R \in [-1, 1]^{d_\theta \times d_\theta}$  be a correlation matrix,  $\Phi_R$  denote the joint cdf of a multivariate Gaussian distribution with mean vector 0 and correlation matrix  $R$ , and  $\Phi^{-1}$  be the inverse cdf of a univariate standard normal distribution. The Gaussian copula  $C_R^{\text{Gaussian}}$  is given by

$$C_R^{\text{Gaussian}}(u_1, \dots, u_{d_\theta}) = \Phi_R(\Phi^{-1}(u_1), \dots, \Phi^{-1}(u_{d_\theta})).$$

Define  $\eta = (\eta_1, \dots, \eta_{d_\theta})^T$ , with  $\eta_i = \Phi^{-1}(u_i)$ ,  $i = 1, \dots, u_{d_\theta}$ . Then the Gaussian copula density is given by

$$c_R^{\text{Gaussian}}(u_1, \dots, u_{d_\theta}) = \frac{1}{|R|^{1/2}} \exp\left(-\frac{1}{2}\eta^T(R^{-1} - I)\eta\right),$$

where  $|R|$  denotes the determinant of  $R$  and  $I$  is the identity matrix.

The  $t$ -copula is defined similarly. Let  $t(\nu, 0, R)$  denote a  $d_\theta$  dimensional t distribution with zero mean vector and correlation matrix  $R \in [-1, 1]^{d_\theta \times d_\theta}$ . Let  $F_{R, \nu}^t$  and  $f_{R, \nu}^t$  denote the cdf and pdf of such distribution. Let  $F_{t, \nu}^{-1}$  be the inverse cdf of a univariate  $t$ -distribution with  $\nu$  degrees of freedom. The  $t$ -copula  $C_{R, \nu}^t$  is given by

$$C_{R, \nu}^t(u_1, \dots, u_{d_\theta}) = F_{R, \nu}^t(F_{t, \nu}^{-1}(u_1), \dots, F_{t, \nu}^{-1}(u_{d_\theta})),$$

with copula density given by

$$c_{R, \nu}^t(u_1, \dots, u_{d_\theta}) = \frac{f_{R, \nu}^t(F_{t, \nu}^{-1}(u_1), \dots, F_{t, \nu}^{-1}(u_{d_\theta}))}{\prod_{i=1}^{d_\theta} f_{\nu}^t(F_{t, \nu}^{-1}(u_i))}.$$

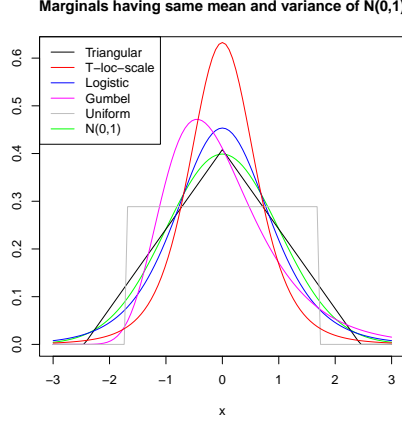


Figure 10: Probability density plots of the triangular (black), location-scale  $t$  (red), logistic (blue), Gumbel (magenta) and uniform (gray) distributions with same mean and variance of the standard normal (green).

## C Appendix C

**$t$ -location scale distribution.** If  $X_j$  follows a  $t$ -location scale distribution with degrees of freedom  $\nu > 0$ , location parameter  $\mu \in \mathbb{R}$  and scale parameter  $\sigma > 0$ , its mean and variance are given by  $\mu$ , for  $\nu > 1$  and  $\sigma^2 \frac{\nu}{\nu-2}$ , for  $\nu > 2$ , respectively. Setting  $\mathbb{E}[X_j] = m_j^*$  and  $\text{Var}(X_j) = S_{jj}^*$ , we get

$$\mu = m_j^*, \quad \sigma^2 = \frac{\nu - 2}{\nu} S_{jj}^*,$$

where  $\nu$  can be chosen arbitrarily .

**Logistic distribution.** If  $X_j$  follows a logistic distribution with location parameter  $\mu \in \mathbb{R}$  and scale  $s > 0$ , its mean and variance are given by  $\mu$  and  $\frac{1}{3}s^2\pi^2$ , respectively. Setting  $\mathbb{E}[X_j] = m_j^*$  and  $\text{Var}(X_j) = S_{jj}^*$ , we get

$$\mu = m_j^*, \quad s = \sqrt{3S_{jj}^*/\pi}.$$

**Normal distribution.** If  $X_j$  follows a Gaussian distribution with parameters  $\mu_j, \sigma_j^2$ , we set  $\mu_j = m_j^*$ ,  $\sigma_j^2 = S_{jj}^*$ .

**Triangular distribution.** If  $X_j$  follows a triangular distribution in  $[a, b]$ ,  $a \leq b$  with mode  $c \in [a, b]$ , its mean and variance are given by

$$\mathbb{E}[X_j] = \frac{a + b + c}{3}, \quad \text{Var}(X_j) = \frac{a^2 + b^2 + c^2 - ab - ac - bc}{18}.$$

Setting  $c = m_j^*$ ,  $\mathbb{E}[X_j] = m_j^*$  and  $\text{Var}(X_j) = S_{jj}^*$  we get

$$a = m_j^* - \sqrt{6S_{jj}^*}, \quad b = m_j^* + \sqrt{6S_{jj}^*}, \quad c = m_j^*.$$

**Uniform distribution.** If  $X_j$  follows a uniform distribution in  $[a, b]$ , its mean and variance are given by  $\mathbb{E}[X_j] = \frac{1}{2}(a + b)$ ,  $\text{Var}(X_j) = \frac{1}{12}(b - a)^2$ . Setting  $\mathbb{E}[X_j] = m_j^*$  and  $\text{Var}(X_j) = S_{jj}^*$ , we get

$$a = m_j^* - \sqrt{3S_{jj}^*}, \quad b = m_j^* + \sqrt{3S_{jj}^*}.$$

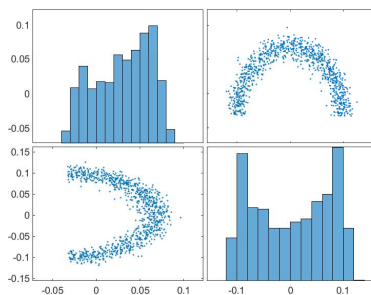


Figure 11: Two-moons: scatter plot matrix of 1,000 summaries simulated with  $\theta_1 = 0.2$  and  $\theta_2 = 0.2$ . The diagonal reports the histogram for each dimension of the summary statistics and the other entries give the pairwise associations.

## Supplementary Material

### C.1 Vectorised computation of the weighted covariance matrix for $(s, \theta)$

The weighted covariance matrix  $S$  given in equation (4) of the main text can be efficiently computed in a vectorized way as follows. Following the same notation established in that section, say that  $x^{(i)} = (\theta^{(i)}, s^{(i)})$  is  $d$ -dimensional and  $i = 1, \dots, N$ . Now call  $\mathbf{x}$  the  $d \times N$  matrix whose  $i$ -th column is  $x^{(i)}$ , and use  $'$  to denote transposition and  $\mathbf{w}$  to denote the  $(1 \times N)$ -dimensional vector of normalised weights. Use  $*$  to denote matrix multiplication and  $.*$  for element-wise multiplication. Then we have the following Matlab code, which can easily be adapted to other languages:

```
weigh_mean = w * x';
S = x' - repmat(weigh_mean, N, 1);
S = S' * (S .* repmat(w', 1, d));
S = S ./ (1-sum(w.^2));
S = 0.5 * (S + S');
```

The resulting  $S$  is of course a  $d \times d$  matrix. The last line in the code is optional but typically useful when small floating-point approximations make  $S$  not exactly symmetric.

### C.2 Two-moons model: simulated summaries distribution and running times for the copula-based samplers

For the two-moons model, the two-dimensional summary statistics are the simulated data themselves, see Figure 11. In Table 2, we report the wallclock times of the copula-based methods to produce ten runs with the Gaussian and t copulas and the six considered marginals. In terms of times, except for the case of Gumbel marginals, the approaches driven by the Gaussian copula are faster than those based on the t copula.

### C.3 Recruitment boom-and-bust: simulated summaries distribution, results for t-copulas and ESS

Figure 13 reports the ESS for all approaches. Figure 14 reports scatter plots of simulated summaries generated conditionally on ground-truth parameters. Figure 15 reports ABC marginal posteriors obtained with all methods and t-copulas, similarly to Figure 6 where Gaussian copulas were chosen instead.

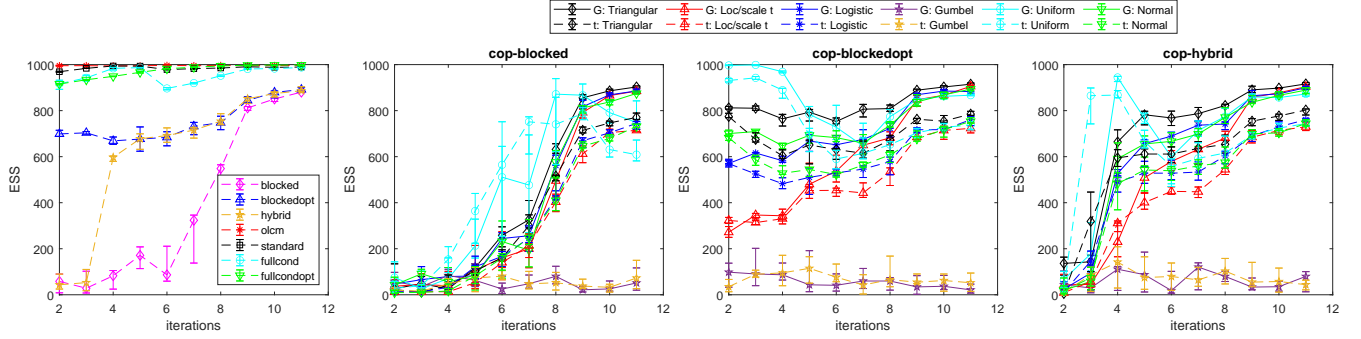


Figure 12: Two-moons: median acceptance rates and error bars with first and third quartile across ten independent runs at each iteration. (Left panel) Non-copula based methods, both guided and not-guided; (center-left) `cop-blocked`; (center-right) `cop-blockedopt`, (right) `cop-hybrid`. The copula-based methods are derived using either Gaussian (G) or t copulas for different marginals, as described in the legend.

	Gaussian copula						t copula					
	Tr	LoScT	Log	Gum	Unif	Norm	Tr	LoScT t	Log	Gum	Unif	Norm
<code>cop-blocked</code>	35.0	52.5	43.1	27.2	3.4	8.1	35.5	56.2	48.3	19.2	3.2	11.3
<code>cop-blockedopt</code>	34.1	49.8	43.8	30.2	9.2	11.4	43.7	71.2	59.6	25.1	12.0	13.8
<code>cop-hybrid</code>	37.4	54.6	45.9	23.5	8.5	9.4	39.1	54.9	48.5	22.6	11.2	12.8

Table 2: Two-moons: Total wallclock times (minutes) for ten runs of the `cop-blocked`, `cop-blockedopt` and `cop-hybrid` approaches with triangular (tr), location-scale t (LoScT), logistic (Log), Gumbel (Gum), uniform (Unif) and normal (Norm) marginals.

#### C.4 Twisted prior study: fullcondopt with joint sampling of two components

Here we illustrate how to construct a version of `fullcondopt` for the 5-dimensional parameter  $\theta$  considered in the twisted-prior model. Each component  $\theta_3$ ,  $\theta_4$  and  $\theta_5$  is proposed from a corresponding 1-dimensional Gaussian as illustrated in section 3.2 of the main paper. However for given  $\theta^* = (\theta_1^*, \dots, \theta_5^*)$  we wish to propose  $\theta_{(1,2)}^{**} = (\theta_1^{**}, \theta_2^{**})$  jointly from  $q(\theta_{1,2}^{**} | \theta_{3,4,5}^*, s_y)$ , that is  $\theta_{(1,2)}^{**}$  is proposed in block, and this is why in the main paper we called this version `fullcondoptblocked`. We have the  $2 \times 1$  column vector (all column vectors are stacked)

$$\hat{m}_{(1,2)|s_y,t-1} = \begin{bmatrix} \hat{m}_1 \\ \hat{m}_2 \end{bmatrix} + \hat{S}_{(1,2),-(1,2)} (\hat{S}_{-(1,2),-(1,2)})^{-1} \left( \begin{bmatrix} \theta_3^* \\ \theta_4^* \\ \theta_5^* \\ s_y \end{bmatrix} - \begin{bmatrix} \hat{m}_3 \\ \hat{m}_4 \\ \hat{m}_5 \\ \hat{m}_s \end{bmatrix} \right). \quad (17)$$

Then we have the  $2 \times 2$  covariance matrix

$$\hat{\Sigma}_{(1,2),t} = \sum_{l=1}^{N_0} \gamma_{t-1,l} (\tilde{\theta}_{t-1,(1,2),l} - \hat{m}_{(1,2)|s_y,t-1}) (\tilde{\theta}_{t-1,(1,2),l} - \hat{m}_{(1,2)|s_y,t-1})'.$$

Then  $q(\theta_{1,2}^{**} | \theta_{3,4,5}^*, s_y) \equiv \mathcal{N}(\hat{m}_{(1,2)|s_y,t-1}, \hat{\Sigma}_{(1,2),t})$ . Overall, the full perturbed  $\theta^{**} = \theta_{(1,\dots,5)}^{**}$  is proposed from (with notation abuse)

$$q(\theta^{**} | \theta^*, s_y) = \mathcal{N}(\hat{m}_{(1,2)|s_y,t-1}, \hat{\Sigma}_{(1,2),t}) \times \prod_{k=3}^5 \mathcal{N}(\hat{m}_{k|s_y,t-1}, \hat{\sigma}_{k|s_y,t-1}^2),$$

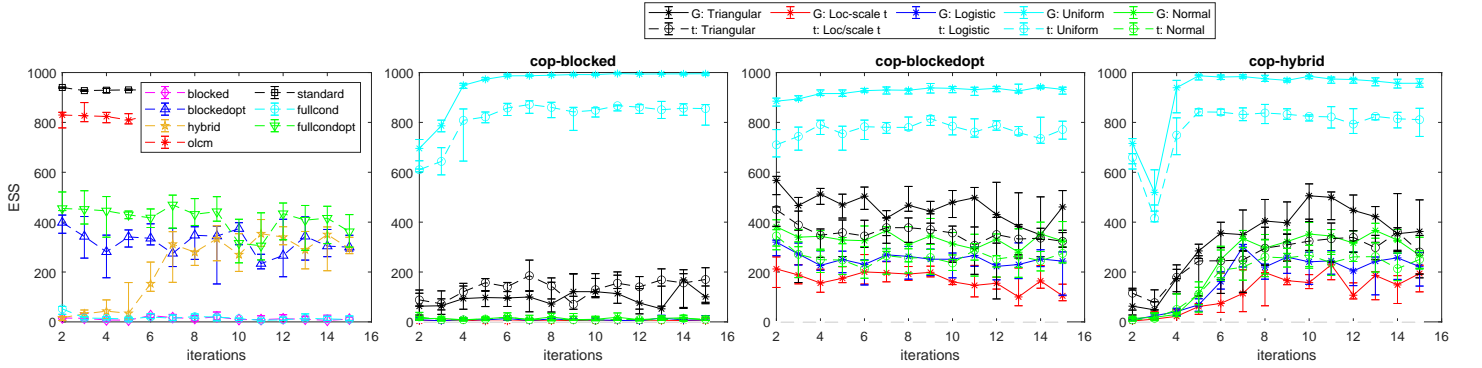


Figure 13: Boom-and-bust model: median ESS and error bars with first and third quartile across ten independent runs at each iteration. (Left panel) Non-copula based methods, both guided and not-guided; (center-left) `cop-blocked`; (center-right) `cop-blockedopt`, (right) `cop-hybrid`. The copula-based methods are derived using either Gaussian (G) or t copulas for different marginals, as described in the legend.

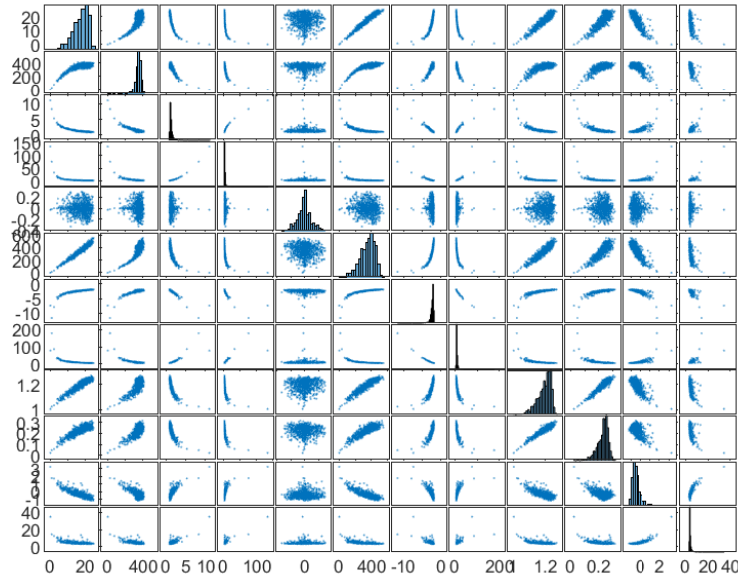


Figure 14: Boom-and-bust model: scatter plot matrix of 1,000 summaries simulated with  $r = 0.4$ ,  $\kappa = 50$ ,  $\alpha = 0.09$  and  $\beta = 0.05$ . The diagonal reports the histogram for each dimension of the summary statistics and the other entries give the pairwise associations.

where the  $\mathcal{N}(\hat{m}_{k|s_y,t-1}^*, \hat{\sigma}_{k|s_y,t-1}^2)$  are as in section 3.2.

### C.5 Twisted model: acceptance rates

In Figure 16, we report the median acceptance rates at each iteration obtained on ten independent runs for all methods applied to the twisted model. All methods are equivalent at the first iteration,

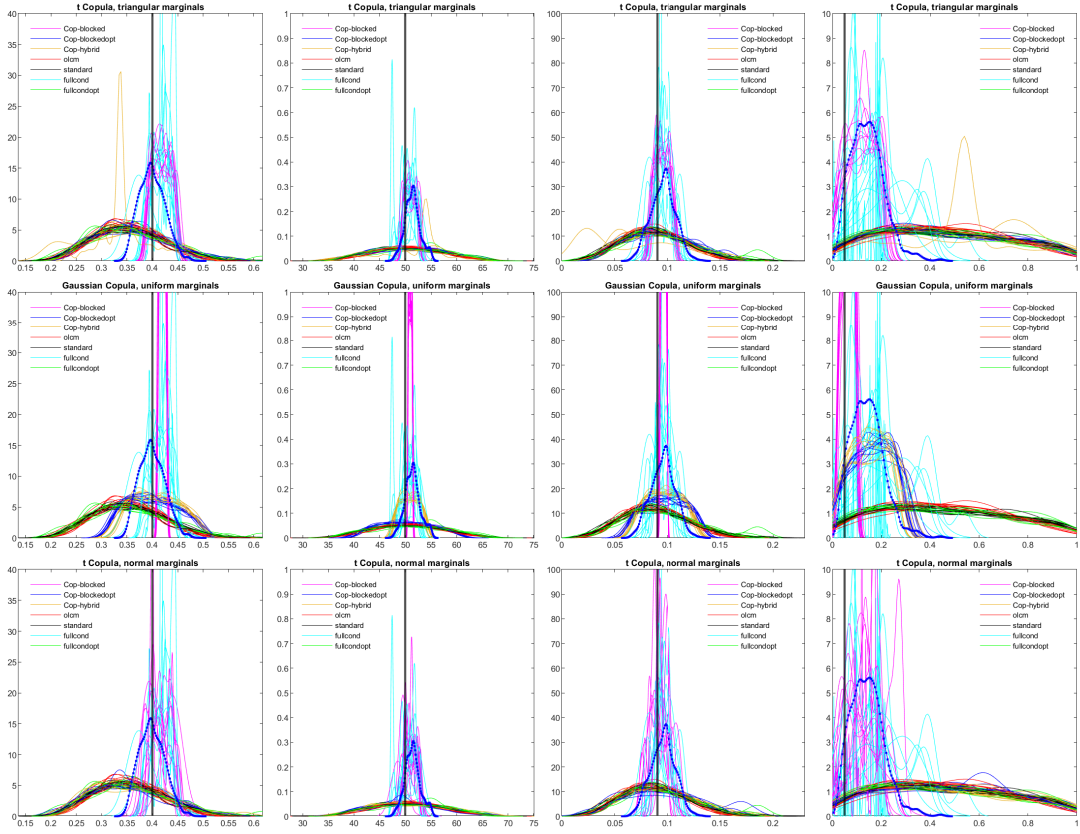


Figure 15: Boom-and-bust model: marginal posterior densities at the last iteration in all ten estimation runs obtained with all methods and t copulas with triangular, uniform and normal marginals. True parameters value are denoted by the vertical lines. Robust semiBSL (blue); copula-blocked (magenta); copula-blockedopt (gray); copula-hybrid (orange); olcm (red); standard (black); fullcond (cyan); fullcondopt (green).

as accepted draws are all proposed from the prior. All guided approaches have a higher acceptance rate at the second iteration (left panel), around 8-13%, while olcm has around 2% acceptance and standard has about 0.1% acceptance rate. At iteration 3, guided methods have between 1.5-2% acceptance rates while the non-guided ones recover towards a 3% acceptance rate, and afterwards all methods stabilize towards similar acceptance rates, with the copula-based approaches with triangular marginals having slightly higher acceptance rates than the corresponding normal ones. In the main text, we suggested that we could have stopped the inference once the acceptance rates turned smaller than 1.5% for two consecutive iterations. We verified that, and for this stopping criterion, the method fullcondoptblocked (recall this is fullcondopt with  $(\theta_1, \theta_2)$  proposed in block using the method in supplementary section C.4) returned a much improved inference than that portrayed for the last iteration in Figure 17, see instead Figure 19. Similar results are obtained when stopping the methods once the acceptance rate has gone below 1% for the second consecutive time, see Figure 18.

## C.6 Hierarchical g-and-k model

Here we display some results obtained with olcm, corresponding to inference obtained using about 1 millions simulations (same as hybrid). The marginal posteriors are in Figure 22. While this is an

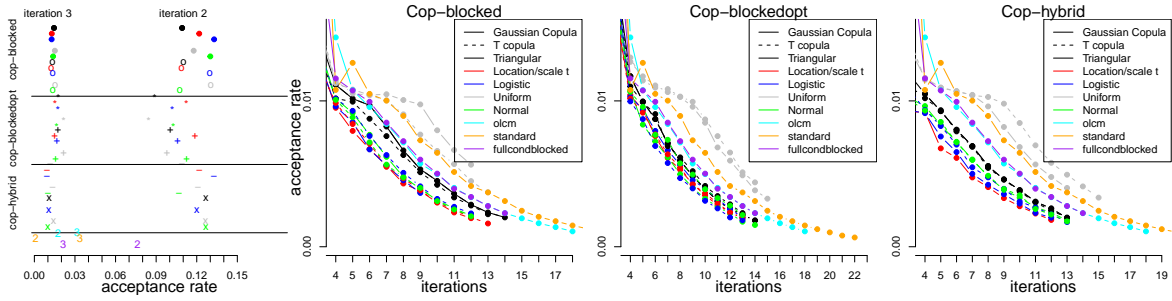


Figure 16: Twisted model: Median acceptance rates across ten independent runs for `olcm` (cyan), `standard` (orange), `fullcondoptblocked` (purple), `cop-blocked` (left panel, top strip and left-center panel), `cop-blockedopt` (left panel, middle strip and right-center panel) and `cop-hybrid` (left panel, bottom strip and right panel), with Triangular (black), Location/scale  $t$  (red), Logistic (blue), Uniform (gray) and Normal marginals (green) distributions. Left panel: iterations 2 and 3 for all methods. The copula approaches are based on Gaussian (top five points in each strip) and  $t$  copulas (bottom five points in each strip).

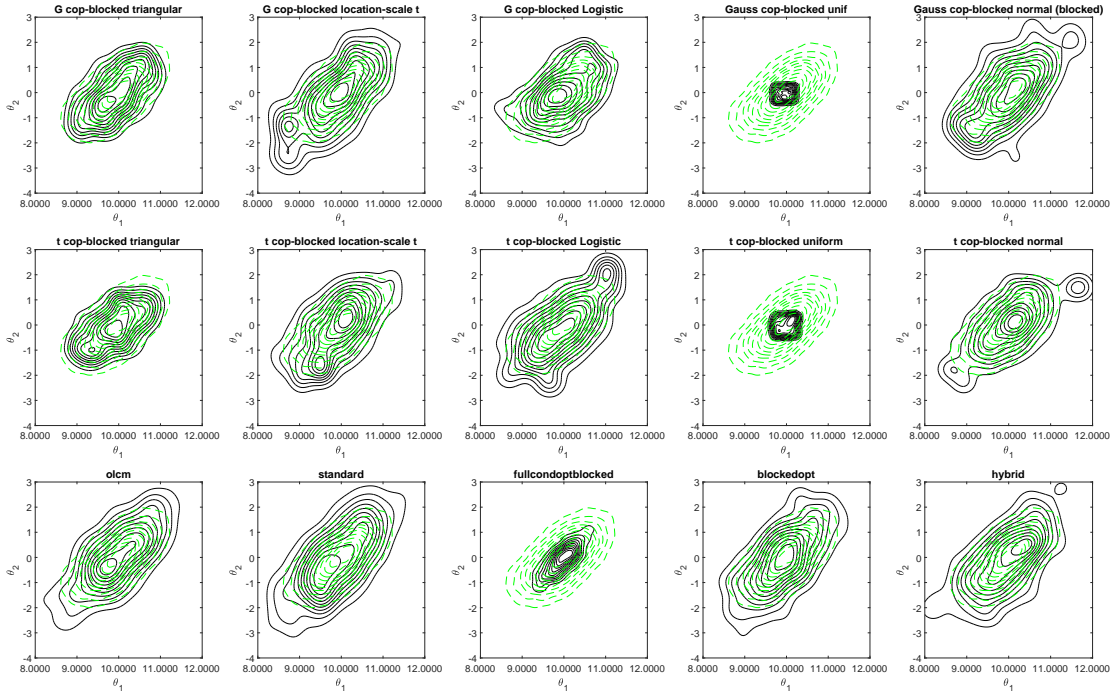


Figure 17: Twisted: Contour plots of the marginal ABC posteriors (black lines) and the exact MCMC posteriors (dashed green lines) of  $(\theta_1, \theta_2)$  at the last iteration in one of the ten runs. Notice, for some methods the results obtained at the last iteration does not necessarily correspond to the best inference (according to the Wasserstein distance). This happens for example for `fullcondopt` with blocked  $(\theta_1, \theta_2)$  (third row and third column). Compare with Figure 7 in the main text.

improvement over results from `standard`, posterior uncertainty is still large and the run took 9 hours, against the 6 minutes of a run with the guided `hybrid`. We can also see in Figure 23 that even after 16 million iterations and 55 hours of computation the `olcm` posteriors are wider than ABC-Gibbs (and `hybrid` as shown in the main text).

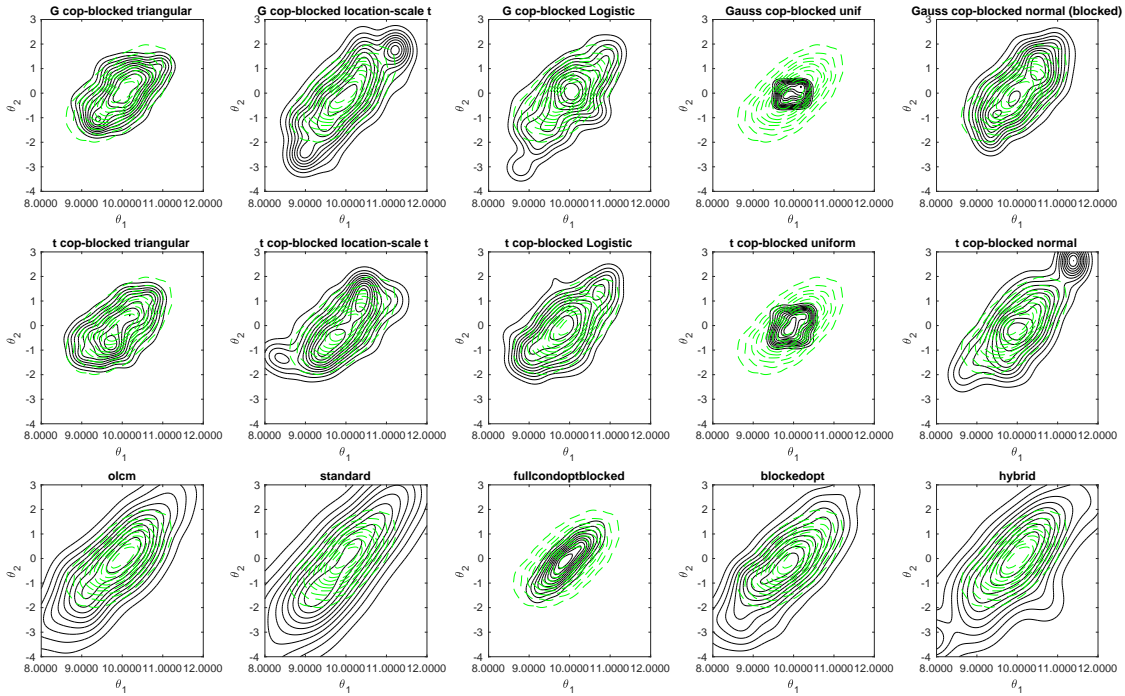


Figure 18: Twisted: Contour plots of the marginal ABC posteriors (black lines) and the exact MCMC posteriors (dashed green lines) of  $(\theta_1, \theta_2)$  at the iteration when the acceptance rate goes below 1% for the second consecutive time.

## C.7 Cell motility and proliferation

What is shown in Price et al. (2018) is that their BSL methodology (standing for Bayesian synthetic likelihood), which is based on MCMC sampling, produces more accurate inference than an ABC-MCMC sampler, and in their work both are initialized essentially at ground-truth parameters, hence a greatly simplified scenario. Here we show that while our samplers are of course not initialised a ground truths, the considered size for the summaries is not really a problem for ABC when SMC samplers are considered, and we manage to obtain much more accurate inference than their ABC-MCMC implementation. Their Matlab code is publicly available in the cited reference, and this enabled us to use the same model simulator, summary statistics and data. We provide a short description of the model and data, extrapolated from Price et al. (2018), where the interested reader is directed for further details.

Cell motility and proliferation are important parts of many biological processes. Cell motility causes random movement, which, together with proliferation or reproduction, can cause tumors to spread or wounds to heal. In real-life experiments, to create the observed data, the cells can be placed on a two-dimensional discrete lattice using image analysis software and some manual intervention. However here we consider simulated data. Cells are motile, with the ability to randomly move to a neighboring lattice site, so cells are equally likely to attempt movement in the four directions of a two-dimensional surface (north, east, south, west). If the attempted movement is to a vacant site, then the motility event is successful. The movement is modelled using random walks in the four directions, and can be parametrized via the probability of motility and proliferation,  $P_m$  and  $P_p$  respectively. These are the parameter of interest for us. Let  $X_{x,y}^t \in \{0, 1\}$  be an indicator that defines whether a cell is present at position  $(x, y)$  for  $x \in \{1, \dots, R\}$ ,  $y \in \{1, \dots, C\}$  at time index  $t \in \{0, 1, \dots, 144\}$ , which means every 5 minutes for 12 hours. Here  $R$  and  $C$  are the number of rows and columns in the lattice,

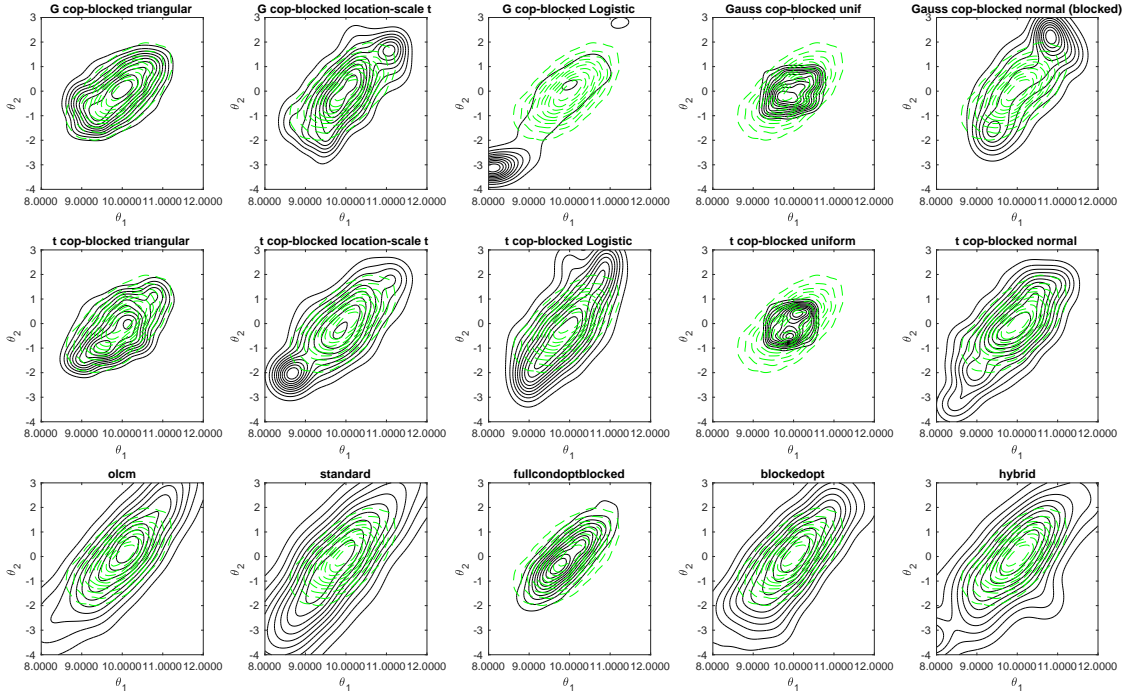


Figure 19: Twisted: Contour plots of the marginal ABC posteriors (black lines) and the exact MCMC posteriors (dashed green lines) of  $(\theta_1, \theta_2)$  at the iteration when the acceptance rate goes below 1.5% for the second consecutive time.

respectively. Denote the matrix of indicators at time index  $t$  as  $X^t$ . Price et al. (2018) consider the Hamming distance between  $X^t$  and  $X^{t-1}$  as an informative summary statistic regarding motility, and this is given by

$$s_t = \sum_{x=1}^R \sum_{y=1}^C |X_{x,y}^t - X_{x,y}^{t-1}|.$$

The summary statistic used to provide information regarding the proliferation is the total number of cells at the end of the experiment, denoted as  $K$  for some simulated dataset. Thus, the vector of summary statistics is given by  $s = (s_1, \dots, s_{144}, K)$  and has dimension 145. The data are simulated with  $P_m = 0.36$  and  $P_p = 0.001$ , with  $R = 27$  and  $C = 36$ . Initially, 110 cells are placed randomly in the rectangle with positions  $x \in \{1, 2, \dots, 13\}$  and  $y \in \{1, 2, \dots, 36\}$ .

We compare our guided schemes with `olcm` and BSL (specifically the version denoted `uBSL` in Price et al., 2018, but we keep writing BSL for simplicity). BSL is run using their provided code, where at each proposed parameter 5,000 model simulations are independently simulated, and we run BSL for 5,000 iterations (hence a total 25 million simulations from the model), starting it at  $P_m = 0.30$  and  $P_p = 0.001$ , with a code running in parallel on a computer node with four cores. For all experiments we set priors  $P_m \sim U(0, 1)$  and  $P_p \sim U(0, 1)$ . Notice that the version of BSL that we run is the original (vanilla) one, simply meant to replicate the results in Price et al. (2018), but it should be possible to reduce the computational demands, see below. Same as in the other case studies, before starting the ABC procedures we simulate summaries from the prior predictive (10,000 times in this example), and compute their MAD. No further tuning is applied to our algorithms, and in all cases the initial threshold was set to  $\delta_1 = 788$  and was automatically decreased as in previous sections, using  $\psi = 1$ . We used  $N = 1,000$  particles.

Figure 24 shows the performance of SMC-ABC across four iterations of `olcm` and the guided `hybrid`

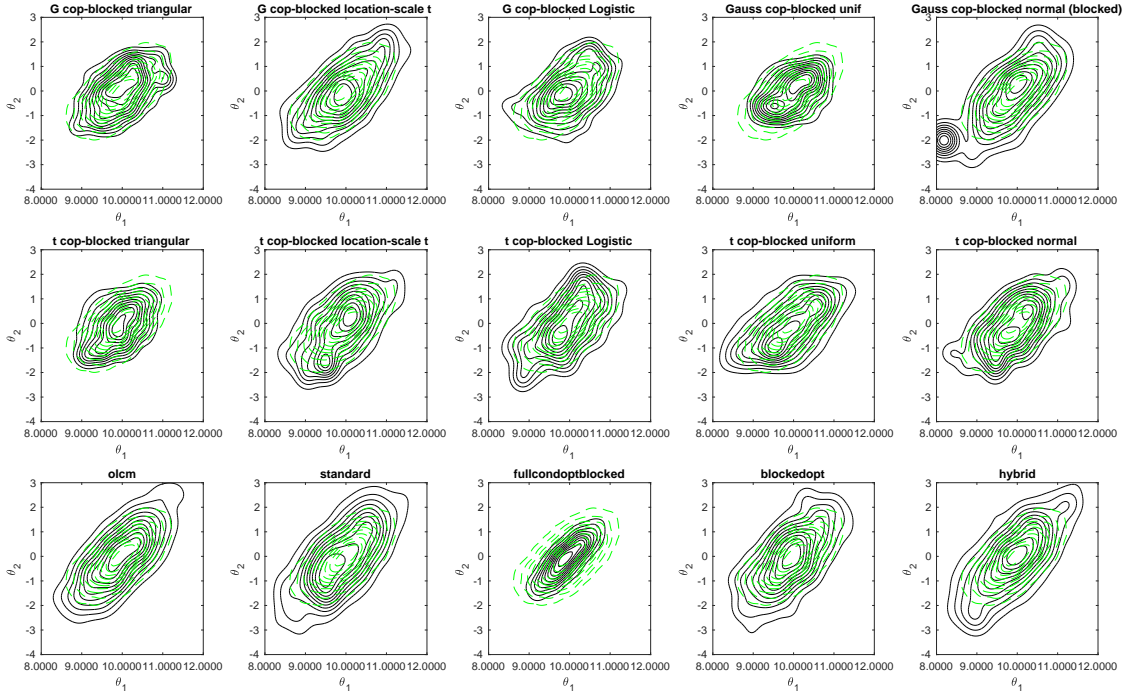


Figure 20: Twisted: Contour plots of the marginal ABC posteriors (black lines) and the exact MCMC posteriors (dashed green lines) of  $(\theta_1, \theta_2)$  at the iteration yielding the smallest log-Wasserstein distance, see Figure 7.

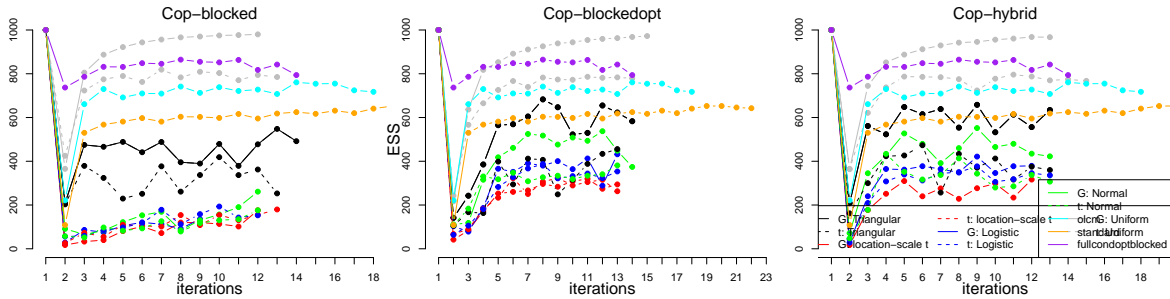


Figure 21: Twisted model: median ESS with first and third quartile across ten independent runs at each iteration. Left panel: `cop-blocked`; centre panel: `cop-blockedopt`, right panel: `cop-hybrid`. The copula-based methods are derived using either Gaussian (G, continuous lines) or t copulas (t, dashed lines) for different marginals, as described in the legend. In all panels, we also report the non-guided `olcm` (cyan) and `standard` (orange), and the guided `fullcondoptblocked` (purple).

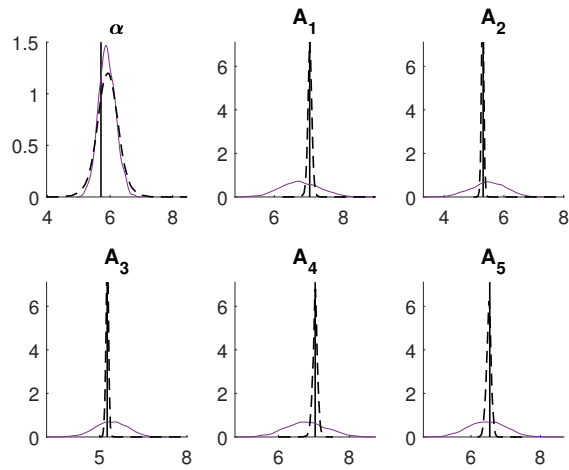


Figure 22: Hierarchical g-and-k: posteriors for  $(\alpha, A_1, \dots, A_5)$  from `o1cm` after 1 million model simulations (at iteration  $t = 22$  we obtained  $\delta = 1.87$ ) which took about 9 hours. Dashed lines are marginals from ABC-Gibbs. Black vertical lines mark ground-truth values.

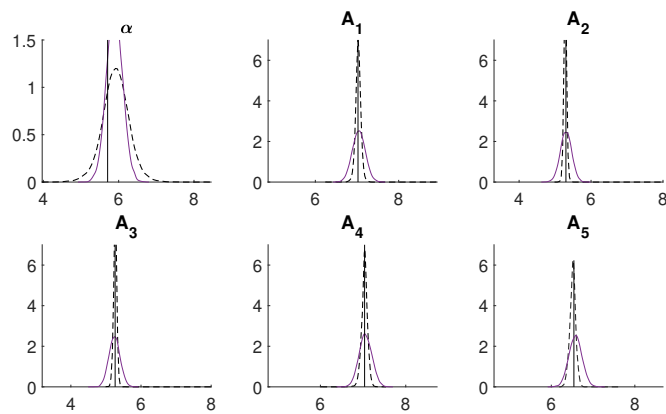


Figure 23: Hierarchical g-and-k: posteriors for  $(\alpha, A_1, \dots, A_5)$  from `o1cm` after 16 million model simulations (at iteration  $t = 41$  we obtained  $\delta = 0.70$ ) which took about 55 hours. Dashed lines are marginals from ABC-Gibbs. Black vertical lines mark ground-truth values.

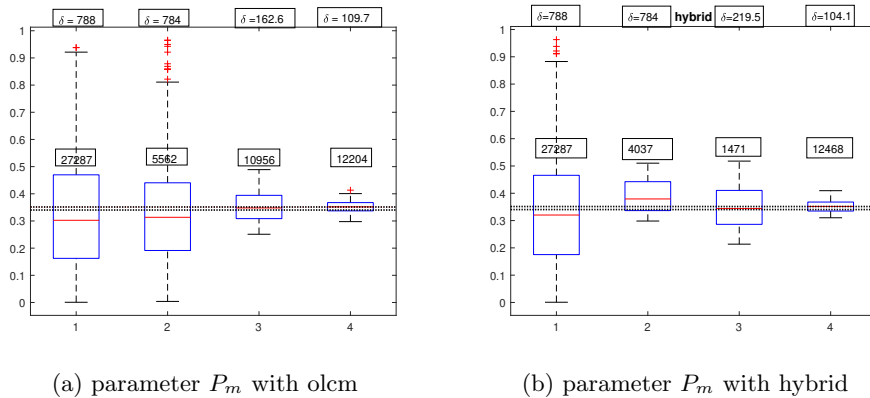


Figure 24: Cell model using 145 summaries: evolution of the marginal posterior for  $P_m$  across four iterations of SMC-ABC when using (a) `olcm`; (b) `hybrid`. The headings report the tolerance values for each iteration. The numbers just above the boxplots are the number of model simulations performed at the corresponding iterations. The dotted horizontal lines are the 25-75 percentiles of the BSL marginals.

method. We notice that `hybrid` reaches a smaller threshold ( $\delta_4 = 104.1$ ) than `olcm` ( $\delta_4 = 109.7$ ), and it does it while using a smaller total number of model simulations for the four iterations, equal to 45,623 whereas `olcm` produced 56,009 model simulations in total. The inference at the last iteration appears satisfying for both methods, see Figure 25, despite the “curse of dimensionality” afflicting ABC algorithms when the dimension of  $s_y$  is large. On our desktop computer `hybrid` completed four iterations within 113 seconds while `olcm` required 155 seconds. The considered setup for BSL

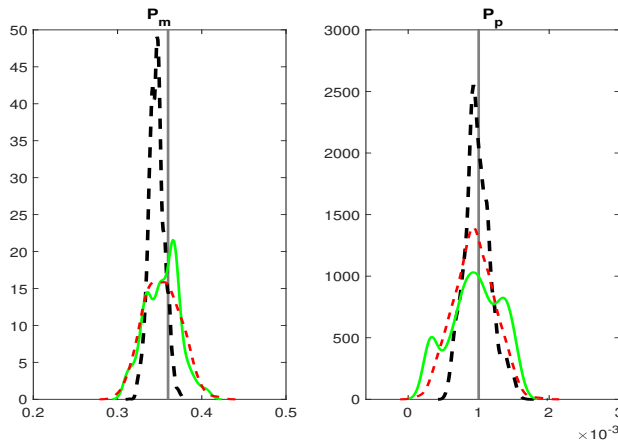


Figure 25: Cell model using 145 summaries: marginal posteriors for BSL (black dashed, after a total of 25 million model simulations), `olcm` (red, after a total 56,009 model simulations and  $\delta_4 = 109.7$ ), guided `hybrid` (green, after a total 45,263 model simulations and  $\delta_4 = 104.1$ ). Vertical lines mark ground truth parameters.

required 16.6 hours for completion, however notice there exists research towards significantly reduce its computational demands, see for example Everitt (2017), Priddle et al. (2021), An et al. (2019) and Picchini et al. (2022). For example An et al. (2019) shows that, by applying an appropriate adjustment to the original BSL procedure, for this case-study it is possible to use 500-1,000 model simulations per iteration, instead of 50,000. The focus of our comparison with BSL here is in terms of

the produced posterior inference rather than accurate time comparisons with the best possible version of BSL. In section C.7.1 we consider a more challenging version of this experiment using more than 400 summary statistics, and in this case inference via SMC-ABC is possible whereas vanilla BSL could not produce any inference even when using 10,000 model simulations per MCMC iteration, and despite the initialization of BSL at ground-truth parameters.

### C.7.1 Cell model: results with more than 400 summaries

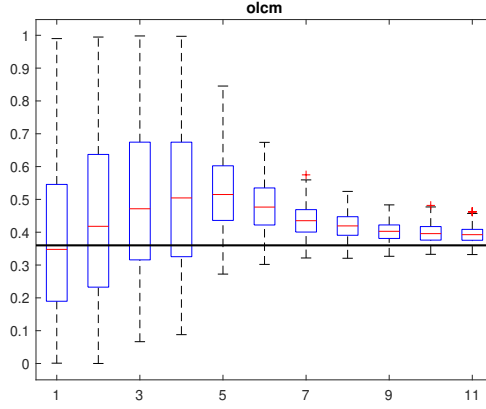
Here we record cells positions for a longer time frame than for the previously considered case. We first consider BSL applied to the case where images are recorded every 5 minutes for a total of 24 hrs, this implying that  $s_y$  has dimension 289. The BSL sampler (vanilla version of Price et al., 2018) was again initialised at the same starting parameters as in the previous section, but here it was unable to mix even with 10,000 model simulations per-iteration, and showing a very high rejection rate with the chains occasionally moving but often stuck for hundreds of iterations in the same position. Essentially inference was unusable. On the opposite side, sequential ABC strategies are able to handle this larger dimension. In fact we are actually going to consider even larger dimensions: using the same ground-truth parameters, we simulate the case where cells positions are recorded every 5 minutes for 36 hrs, using the same positions for the 110 initial cells as for the case considered in the previous section. The resulting  $s_y$  has now dimension 433. We still use  $N = 1,000$  but, since the dimension of the summaries is larger, it is prudent to employ a less aggressive decreasing schedule for  $\delta$ , and here we use  $\psi = 25$  (the 25th percentile). We start with  $\delta_1 = 8,085$  and produce 11 iterations of SMC-ABC with the `olcm` and guided `hybrid` sampler. The samplers behaviour for the parameter  $P_m$  is illustrated in Figure 26. Across the 11 iterations `olcm` simulated from the model 171,778 times for a total of 35 minutes, whereas `hybrid` simulated 175,091 times also for a total of 35 minutes. Ultimately `hybrid` managed to reach a smaller threshold  $\delta_{11} = 651.8$  whereas `olcm` reached  $\delta_{11} = 696.1$ .

Marginal posteriors at the last iteration are in Figure 27 (for ease of comparison, we keep the same ticks on the x-axes as in Figure 25 in the main text). Interestingly, given the increased summaries dimension we expected the curse-of-dimensionality to kick-in, however this only happens for parameter  $P_m$  which has a wider posterior compared to Figure 25, whereas for  $P_p$  the additional information produces tighter posterior.

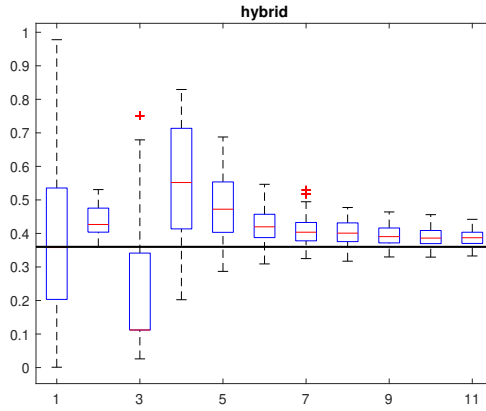
## C.8 Samplers based on a generic distance kernel

In the main paper we focused on considering a uniform kernel to compare simulated and observed summaries, i.e. the 0-1 function  $\mathbb{I}_{\|s^* - s_y\| < \delta}$  for  $s^*$  summaries of simulated data and  $s_y$  summaries of observed data. While this is arguably the most popular choice to compare summaries, it is only one of the possibilities. For the reader’s benefit, here we add a formulations of the basic ABC-rejection, for when a generic kernel is used. For SIS-ABC and SMC-ABC samplers the reader is referred to Fan and Sisson (2018).

A version of ABC-rejection, as given in Wilkinson (2013), proposes parameter  $\theta^*$  generating a distance  $\|s^* - s_y\|$ , then  $\theta^*$  is accepted with probability  $K_\delta(s^*, s_y)/c$  where  $K_\delta$  is an unnormalized kernel and  $c > 0$  is a normalizing constant such that  $c \geq \sup K_\delta(\|\cdot\|)$ . As discussed in Wilkinson (2013), the latter acceptance criterion is equivalent to accepting when  $\|s^* - s_y\| < \delta$ . Typically the kernel is a function of some distance  $\rho = \|\cdot\|$  (e.g. the Euclidean or the Mahalanobis distance), and we expect  $K_\delta(\rho)$  to have a modal value at  $\rho = 0$ , and so taking  $c = K_\delta(0)$  will make the algorithm valid and also ensure efficiency by maximizing the acceptance rate. For full generality, in Algorithm 3 we report the version given in Bornn et al. (2017), where at each proposed parameter  $M \geq 1$  datasets are simulated.



(a) parameter  $P_m$  with olcm



(b) parameter  $P_m$  with hybrid

Figure 26: Cell model using 433 summaries: evolution of the marginal posterior for  $P_m$  across four iterations of SMC-ABC when using (a) olcm; (b) hybrid. The horizontal lines are the ground-truth parameters.

---

**Algorithm 3** Generalized ABC-rejection (Bornn et al., 2017)

---

- 1: **for**  $t = 1$  to  $N$  **do**
  - 2:   **repeat**
  - 3:     Sample  $\theta^* \sim \pi(\theta)$ ,
  - 4:     Simulate  $z^i \sim p(z|\theta^*)$  iid and compute  $s^i = S(z^i)$ ,  $i = 1, \dots, M$ ;
  - 5:     simulate  $u \sim \text{Uniform}(0, 1)$ ;
  - 6:     **until**  $u < \frac{1}{cM} \sum_{i=1}^M K_\delta(s^i, s_y)$
  - 7:     Set  $\theta^{(t)} = \theta^*$
  - 8: **end for**
  - 9: *Output:*
  - 10: A set of parameters  $(\theta^{(1)}, \dots, \theta^{(N)}) \sim \pi_\delta(\theta|s_y)$ .
-

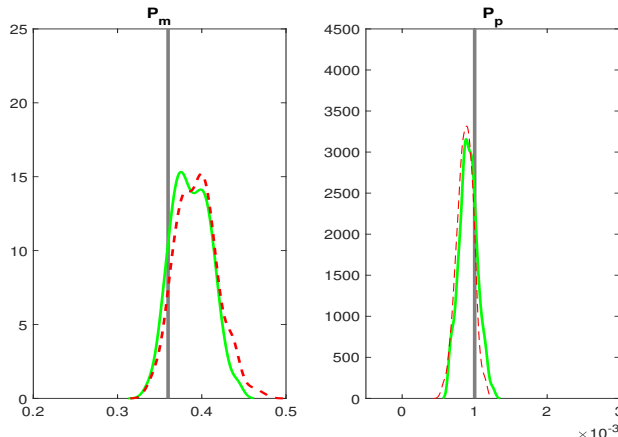


Figure 27: Cell model using 433 summaries: marginal posteriors at the 11th iteration for olcm (red,  $\delta_{11} = 696.1$ ), guided hybrid (green,  $\delta_{11} = 651.8$ ). Vertical lines mark ground truth parameters.

## C.9 Notable proposal samplers for SMC-ABC from background literature

Here, we review some of the proposal samplers for SMC-ABC that provide a useful comparison with our novel methods introduced in section 3 of the main paper. Some of the most notable work for the construction of such samplers is in Filippi et al. (2013). There, for the case where the interest is in constructing samplers based on perturbing a particle randomly picked from the previous set/iteration, they produce ways to tune the covariance matrix of Gaussian proposals that improve on Beaumont et al. (2009). The arguments in both Beaumont et al. (2002) and Filippi et al. (2013) are based on the optimization of a Kullback-Leibler (KL) divergence, where the goal is to obtain a proposal sampler that is maximally similar to the targeted ABC posterior, in a KL sense, and simultaneously maximizes the acceptance probability. See instead Alsing et al. (2018) for a different approach based on obtaining an optimal trade-off between a high acceptance rate and the reduction of the variance of the importance-weights of the accepted samples (hence increasing the effective sample size for the accepted sample).

Beaumont et al. (2009) construct a “component-wise” perturbation kernel that at iteration  $t$  proposes  $\theta^{**}$  by separately perturbing each  $\theta_k^*$  (the  $k$ th components of  $\theta^*$ ) by sampling from the univariate Gaussian proposal

$$q_k(\theta_k|\theta_k^*) \equiv \mathcal{N}(\theta_k^*, \tau_k^2),$$

where  $\theta_k^*$  is the  $k$ th component of  $\theta^*$  and  $\tau_k^2 = 2\sigma_k^2$ , with  $\sigma_k^2$  being the weighted empirical variance of the  $k$ th component of all particles accepted at iteration  $t - 1$ . That this variance should be used in a component-wise approach comes as the optimal solution to the minimization of the KL divergence between the target  $\pi_\delta(\theta|s_y)$  and the proposal kernel. Of course, at time  $t$  all  $d_\theta = \dim(\theta)$  components are perturbed to form  $\theta^{**} = (\theta_1^{**}, \dots, \theta_{d_\theta}^{**})$ . Obviously, the component-wise approach is not particularly appealing when the components of  $\theta$  are correlated in the posterior. A first intuitive amelioration considered in Filippi et al. (2013) is to propose the full  $\theta^{**}$  by generating at iteration  $t$  from the  $d_\theta$ -dimensional Gaussian  $q(\theta|\theta^*) \equiv \mathcal{N}(\theta^*, 2\Sigma)$ , with  $\Sigma$  being the empirical weighted covariance matrix from the particles accepted at iteration  $t - 1$ . This results in the importance weights (1) becoming (with the usual notation abuse)

$$\tilde{w}_t^{(i)} = \pi(\theta_t^{(i)}) / \sum_{j=1}^N w_{t-1}^{(j)} \mathcal{N}(\theta_t^{(i)}; \theta_{t-1}^{(j)}, 2\Sigma_{t-1}), \quad i = 1, \dots, N. \quad (18)$$

In our experiments, this proposal embedded into SMC-ABC is denoted “standard”, being in some way a baseline approach. However, by appealing again to KL optimization arguments, Filippi et al. (2013)

remark that the “standard” sampler is optimal only in the limiting case  $\delta_t = \delta_{t-1} = 0$ . As this is commonly not the case, they derived further improved multivariate Gaussian proposal samplers. One of these considers the “optimal local covariance matrix” (OLCM). The key feature of this sampler is that each proposed particle  $\theta^{**}$  arises from perturbing  $\theta^*$  using a Gaussian having a covariance matrix that is specific to  $\theta^*$  (hence “local”), rather than being tuned on all particles accepted at  $t - 1$ . To construct the OLCM Filippi et al. (2013) define the following weighted set of particles of size  $N_0 \leq N$  at iteration  $t - 1$

$$\{\tilde{\theta}_{t-1,l}, \gamma_{t-1,l}\}_{1 \leq l \leq N_0} = \left\{ \left( \theta_{t-1}^{(i)}, \frac{w_{t-1}^{(i)}}{\bar{\gamma}_{t-1}} \right), \text{ s.t. } \|s_{t-1}^i - s_y\| < \delta_t, \quad i = 1, \dots, N \right\}, \quad (19)$$

where  $\bar{\gamma}_{t-1}$  is a normalization constant such that  $\sum_{l=1}^{N_0} \gamma_{t-1,l} = 1$ . That is, the  $N_0$  weighted particles are the subset of the  $N$  particles accepted at iteration  $t - 1$  (when using  $\delta_{t-1}$ ) having generated summaries that produce distances that are *also* smaller than  $\delta_t$ . To avoid confusion, here we used the letter  $\gamma$  to denote normalised weights associated to the subset of  $N_0$  particles, rather than  $w$ . At iteration  $t$ , the OLCM sampler is defined as a multivariate Gaussian sampler centred at  $\theta^*$  with  $q_t(\theta|\theta^*) = \mathcal{N}(\theta^*, \Sigma_{\theta^*}^{\text{olcm}})$  where

$$\Sigma_{\theta^*}^{\text{olcm}} = \sum_{l=1}^{N_0} \gamma_{t-1,l} (\tilde{\theta}_{t-1,l} - \theta^*) (\tilde{\theta}_{t-1,l} - \theta^*)'.$$

It is clear that each  $\theta^*$  is then perturbed using a covariance matrix that is specific to  $\theta^*$ , unlike the “standard” sampler which uses the same covariance for all perturbed particles. Accepted particles are given unnormalised weights

$$\tilde{w}_t^{(i)} = \pi(\theta_t^{(i)}) / \sum_{j=1}^N w_{t-1}^{(j)} \mathcal{N}(\theta_t^{(i)}; \theta_{t-1}^{(j)}, \Sigma_{\theta^{(j)}}^{\text{olcm}})$$

where

$$\Sigma_{\theta^{(j)}}^{\text{olcm}} = \sum_{l=1}^{N_0} \gamma_{t-1,l} (\tilde{\theta}_{t-1,l} - \theta_{t-1}^{(j)}) (\tilde{\theta}_{t-1,l} - \theta_{t-1}^{(j)})'.$$

Note that the computation of  $\Sigma_{\theta^*}^{\text{olcm}}$  causes some non-negligible overhead in the computations, since it has to be performed for every proposal parameter, and sanity checks on this matrix have to be performed to ensure that this is a proper covariance matrix, otherwise computer implementations will halt with an error. We discuss this in section 3.2. For the implementation of OLCM, we are required to store the  $N$  distances  $\|s_{t-1}^i - s_y\|$  accepted at iteration  $t - 1$ , so that it is possible to determine which indices  $i$  have  $\|s_{t-1}^i - s_y\| < \delta_t$ . OLCM implicitly embeds a stopping criterion for SMC-ABC, as clearly the sampler should stop at iteration  $t$  when the current updated  $\delta_t$  is such that  $N_0 = 0$  (or possibly a positive but “small enough”  $N_0$ , though this aspect is not investigated in Filippi et al., 2013).

Filippi et al. (2013) also introduce further samplers, including one based on nearest neighbors which provided the highest acceptance rate but is computationally more demanding. Ultimately, they recommend OLCM as an acceptable trade-off between sampling efficiency and computational demands.